Tutkimusraportti
Report of Investigation

162

Tapio Ruotoistenmäki and Timo Tervo

Geophysical characteristics of Outokumpu area, SE Finland

GEOMEX Project
A Joint Venture of Geological Survey of Finland and Outokumpu Mining Company
Final Report by Gephysics sub-project

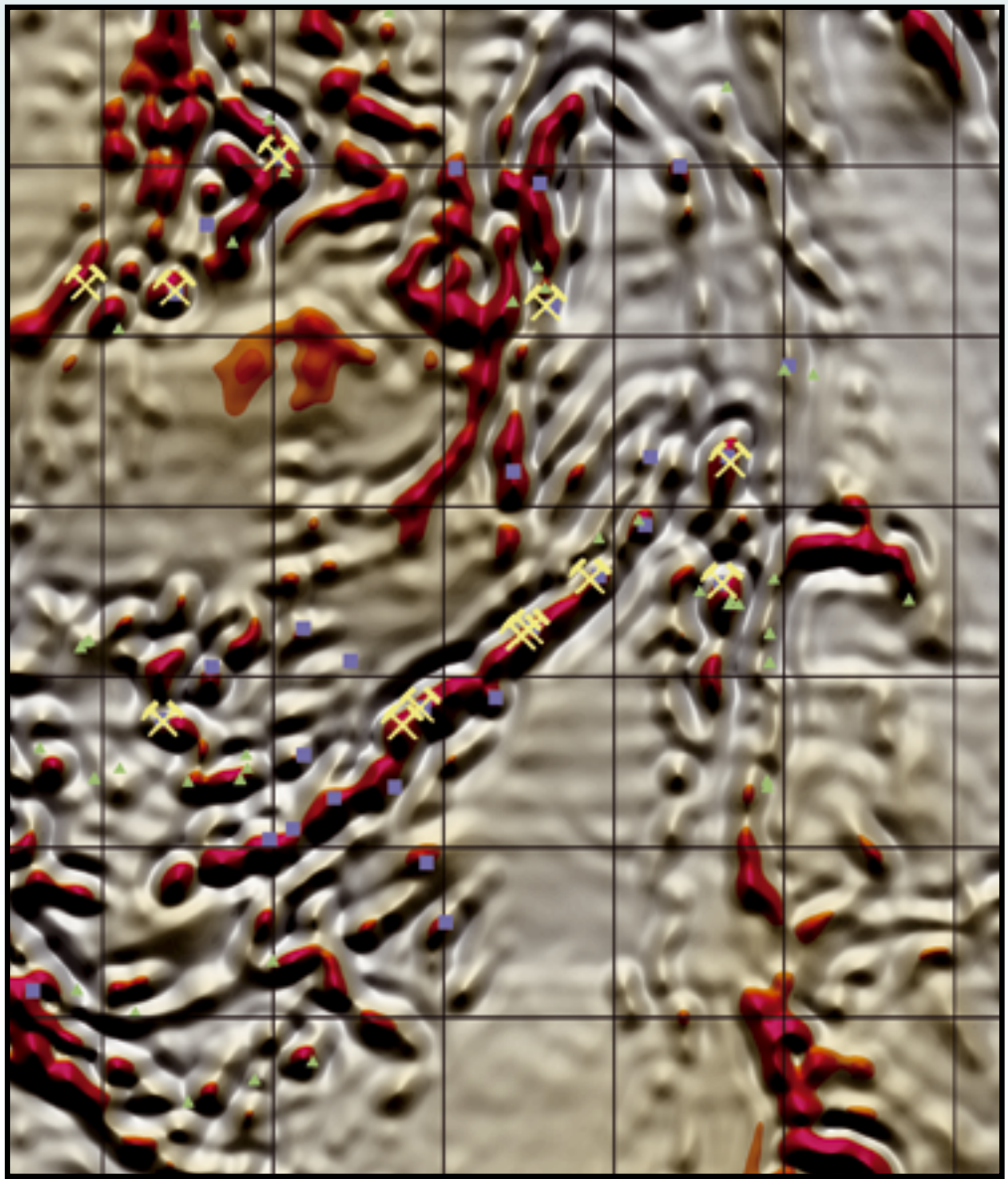

Geological Survey of Finland
Espoo 2006

GEOLOGIAN TUTKIMUSKESKUS **GEOLOGICAL SURVEY OF FINLAND**

Tutkimusraportti 162 Report of Investigation 162

Tapio Ruotoistenmäki and Timo Tervo

GEOPHYSICAL CHARACTERISTICS OF THE OUTOKUMPU AREA, SE FINLAND

Espoo 2006

Ruotoistenmäki, T. 2006. Geophysical Characteristics of the Outokumpu Area, SE Finland. Geologian tutkimuskeskus, Tutkimusraportti – *Geological Survey of Finland, Report of Investigation* 162, 37 pages, 32 figures and 5 tables.

During the years 1998–2003 geological character, evolution and metallogenic potential of the Outokumpu region in Northern Karelia, Finland was reassessed through the Geomex project, which represented a joint venture between the Geological Survey of Finland (GTK) and Outokumpu Mining Oy (OKU). The purpose of the project was to collect, reprocess and archive existing geological and geophysical data and material and locate new target areas for exploration. The main results of the Geomex geophysics sub-project are presented in this paper.

Magnetic and electromagnetic maps were used to define regional tectonic features in the Outokumpu area. The most striking features relate to regional folding with predominantly NE and NW trends forming major interference patterns. The fold structures are also both related to, and truncated by thrust faults. Structural characteristics were studied in further details along key profiles using model interpretations and then correlated with existing deep seismic reflection data.

The long-wavelength component magnetic maps and U/Th radiometric maps were examined with respect to location of currently known sulfide deposits, to provide a basis for defining target areas for future exploration.

The petrophysical data of the GTK database and OKU drill core samples were classified according to their distributions on density – susceptibility diagrams. By this method it was possible to identify rock groups and sub-groups, e.g. various serpentinites, having distinct density – susceptibility combinations. Moreover, the method enabled parameter combinations characteristic of ore potential rock types to be defined.

Key words: (GeoRef Thesaurus, AGI): mineral exploration, geophysical methods, airborne methods, geophysical maps, petrophysics, structural geology, Proterozoic, Outokumpu, North Karelia, Finland

Tapio Ruotoistenmäki
Geological Survey of Finland
PL 96
FIN-02151 ESPOO, FINLAND

E-mail: tapio.ruotoistenmaki@gtk.fi

ISBN 951-690-959-0
ISSN 0781-4240

Vammalan Kirjapaino Oy 2006

Ruotoistenmäki, T. 2006. Geophysical Characteristics of the Outokumpu Area, SE Finland. Geologian tutkimuskeskus, Tutkimusraportti – *Geological Survey of Finland, Report of investigation* 162, 37 sivua, 32 kuvaa ja 5 taulukkoa.

Geologian tutkimuskeskus (GTK) ja Outokumpu Mining Oy (OKU) perustivat vuonna 1998 yhteishankkeen Outokummun alueen geologian ja malmivarojen uudelleenarvioimiseksi. Hankkeen nimeksi tuli Geomex ja se päättyi vuonna 2003. Hankkeen aikana kerättiin, arkistoitiin ja prosessoitiin aiemmin koottu geologinen ja geofysikaalinen aineisto uusien tutkimuskohteiden rajaamiseksi. Geomex-hankkeen geofysiikan osahankkeen oleelliset tulokset esitellään tässä raportissa.

Magneettisia ja sähkömagneettisia karttoja hyödynnettiin määritettäessä Outokummun alueen tektonisia rakennepiirteitä. Merkittävimmät rakenteet liittyvät alueella koillisen ja luoteen suuntaisiin poimuihin, jotka muodostavat paikoin ylityöntösiirrosten leikkaamia alueellisia interferenssirakenteita. Kohteellisesti rakenteita tarkasteltiin yksityiskohtaisemmin tulkitsemalla valittuja magneettisia ja painovoimaprofiileja ja vertaamalla niitä syväseismisiin tulkintoihin.

Pitkäaaltoisten, suodatettujen magneettisten karttojen ja uraani-thorium -suhdekarttojen havaittiin korreloivan merkittävästi malmiesiintymien suhteen, jolloin niitä voi hyödyntää määriteltäessä myös uusia tutkimuskohteita.

GTK:n ja OKU:n petrofysikaaliset näyteaineistot luokiteltiin hyödyntäen niiden suskeptibiliteetti-tiheys -diagrammeja. Menetelmällä voi määrittää eri kivilajiryhmien karakteristiset suskeptibiliteetti-tiheys -kombinaatiot ja niiden malmipotentiaalisuudet.

Asiasanat (GeoRef Thesaurus, AGI): malminetsintä, geofysikaaliset menetelmät, lentomittaukset, geofysikaaliset kartat, petrofysiikka, rakennegeologia, proterotsooinen, Outokumpu, Pohjois-Karjala, Suomi

Tapio Ruotoistenmäki
Geologian tutkimuskeskus
PL 96
02151 ESPOO

Sähköposti: tapio.ruotoistenmaki@gtk.fi

CONTENTS

INTRODUCTION

The Outokumpu Cu-Co-Zn deposit, located in the project area in North Karelia, Finland was discovered in 1910 by tracing a large sulfide-bearing glacial erratic boulder to its source outcrop (Trüstedt, 1921). Since the discovery of the ore, the Outokumpu area has been extensively studied, resulting in numerous publications and (mainly unpublished) reports. In December 1998 the Geological Survey of Finland (GTK) and Outokumpu Mining Oy established the GEOMEX joint venture to conduct geological and geophysical exploration and modeling in the Outokumpu district, and to collect, archive and revise existing data and drill cores. The project consisted of three main sub-projects: Geology, geophysics and data projects, and was completed in 2003. The location and general geology of the project area is shown in Figure 1.

Several geophysical and geological studies and theories on the evolution of the Outokumpu area have been published since the discovery of the Outokumpu ore almost a century ago. In one of the more important works, Gaál et al. (1975) studied the tectonics and stratigraphy of the surroundings of the Outokumpu ore deposit, giving a profound and detailed description of the major ore potential zones in the area. This work was further refined by Koistinen (1981), who concentrated on the details of the structural evolution of the Outokumpu ore deposit and on structures controlling the location of the ore. Park et al. (1984) give a plate tectonic model for the evolution of the Outokumpu as a thrust belt. However, their model remains controversial, as will be shown later in this paper. They interpreted a back arc environment of formation for the Outokumpu assemblage and ore. Mäkelä (1974) inferred a volcanic-exhalative origin for the ore mineralization on basis of sulfur isotopes.

A review of the geological and tectonic evolution of eastern Finland and Outokumpu area geology is given in papers by Sorjonen-Ward (1997), Sorjonen-Ward and Luukkonen (2005) and Tyni et al. (1997). Moreover, a comprehensive summary of publications and up-to-date studies of the area are available from Kontinen and Peltonen (2003).

The ore potential of the Outokumpu area has also been extensively studied by geophysical methods, although most of the results remain unpublished. For example, Rekola and Hattula (1995) describe the geophysical characteristics of the main ore zone and the trend of the ore body in the deeper parts of the zone. Lehtonen (1981) gives a summary of the petrophysical characteristics of the rock types in the Outokumpu ore zone. Airo and Loukola-Ruskeeniemi (2004) studied responses of sulfide deposits and sulfide-rich rocks in airborne magnetic and gamma ray maps of eastern Finland, concentrating particularly on black schists.

In his explanation to the geological map sheet 4221 of Finland Koistinen (1993) described 'thrust sheet tectonics' in the Juojärvi area on SW part of the Outokumpu zone, which resulted in slicing and 'shuffling' of the Outokumpu Nappe and underlying Archaean basement. Thus, it remains uncertain whether the basement domes in the area represent in situ basement or allochthonous sheets detached by thrusting processes. An analysis of deep seismic reflection profiles FIRE-3 measured in the area (Kukkonen et al., 2006) will probably give more information on the deep structures.

To the East the Outokumpu Nappe complex is bordered by Paleoproterozoic Höytiäinen province (see Figure1), considered in detail by Kohonen (1995 and references therein). In his structural model, the Outokumpu Nappe area has been thrusted from W – SW against the Höytiäinen province.

This paper gives a general review of the existing geophysical studies and material from the Geomex-project area, based on the unpublished reports produced by the authors during the project. The main emphasis is on regional scale low-altitude aerogeophysical data and maps. The local scale ground geophysical data, profile studies and interpretation results are given in more detail in our project report (Ruotoistenmäki and Tervo, 2004).

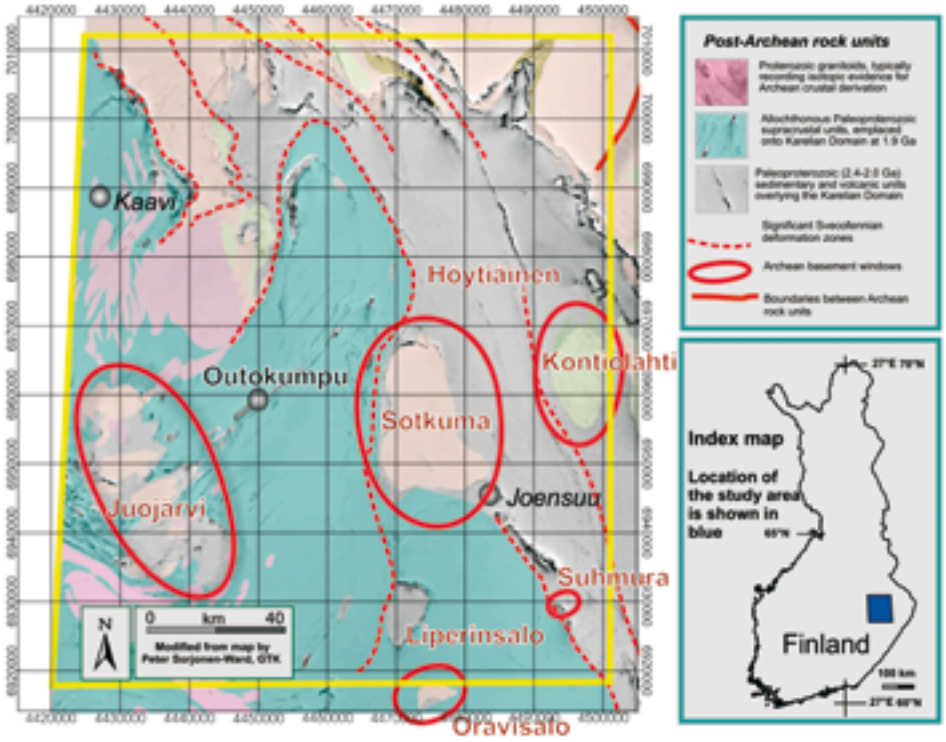

Figure 1. Simplified local scale lithological map of the Geomex project area (outlined by yellow lines). Semitransparent gray shades relate to total magnetic intensity recorded by regional airborne surveys (high anomalies are darker; Reproduced from the Geological Survey of Finland databases). Modified from map by Sorjonen-Ward and Luukkonen (2005).

GEOLOGY AND ORE DEPOSITS

A detailed and most up-to-date description of the geological context and the ore deposits is given by Kontinen and Peltonen (2002, 2003), and is cited in part below:

"The Outokumpu mining camp is located within the North Karelia Schist Belt (NKSB) at the junction of the Neoarchaean Karelian craton in the east and the 1.93–1.80 Ga Paleoproterozoic Svecofennian complex in the west. The NKSB comprises mainly metasedimentary strata, of which the older part, the 2.5–2.0 Ga Jatuli strata, are autochtonous, while the younger 2.0 – <1.92 Ga Kaleva deposits have been to a greater extent thrusted onto the Neoarchaean basement complex. The basement consists mainly of granulite gneisses retrograded to amphibolite facies during Proterozoic. Both, the basement and the NKSB were in western part of the area intruded by 1.87–1.85 Ga syn- to late-kinematic granites.

The Kaleva assemblage in the Outokumpu region consists of two main tectonostratigraphic units. The lower, parautochthonous unit, "lower Kaleva", mainly comprises metaturbiditic graywaces with thin intercalations of low Ti tholeiitic metabasalts and black schists in its upper part. The upper, allochthonous unit, or "upper Kaleva" in the Outokumpu allochthon, mainly comprises deep marine metaturbiditic graywackes with thick intercalations of black schists and sheets and lenses of serpentinized metaperidotite in its basal part.

Single zircon U-Pb age data of the detrital zircons in the psammites in the upper Kaleva assemblage indicate deposition of the unit subsequent to 1.92 Ga (Claesson et al., 1993). The exact timing of thrusting of the Outokumpu allochthon is not known but it can be reasonably inferred to have occurred about 1.90 Ga ago, certainly between 1.92 Ga and 1.87 Ga.

The metasediments of the Kainuu–Outokumpu thrust belt in eastern Finland enclose ultramafic massifs of variable size, interpreted as ophiolites, and distributed over an area of more than 5000 km^2. These bodies, representing fragments of refractory mantle are intimately associated with a) semimassive polymetallic Cu-Co-Zn-Ni-Ag-Au-As sulfide deposits and b) disseminated Ni-sulfide occurrences. The origin of the Cu-Co-Zn-Ni-Ag-Au-As deposits is polygenetic and requires mixing of Cu-Zn-Co sulfides deposited far from any sources of crustal lead at c. 1.95 Ga, with Ni-disseminations that formed concurrent with carbonate-silica alteration at the margins of ultramafic massifs during obduction at ca. 1.90 Ga. Field evidence suggests that the mixing, homogenisation and upgrading of these proto-ores to produce the polymetallic Outokumpu-type ore deposits took place during pervasive tectonic-metamorphic, structurally controlled remobilisation of the sulfides."

GEOPHYSICAL DATA AND MAPS

Between 1951 and 1972 the Geological Survey of Finland (GTK) carried out airborne geophysical surveys covering all of the onshore territory of Finland with flight altitude of ca. 150 metres and line separation of ca. 400 metres. In 1972 GTK commenced a program of airborne mapping at a lower altitude, at a height of ca. 30 – 40 metres and using a denser, ca. 200 m line spacing. Measured geophysical parameters were Earth's total magnetic field, electromagnetic field and gamma radiation (U, Th, K and total). For more details, see Peltoniemi (1982, 2005) and Hautaniemi et al. (2005).

Magnetic maps

Magnetic anomalies and the most important mines in the survey area are shown in Figure 2. Long linear anomaly zones are generally related to the traces of thrust surfaces separating overlapping thrust sheets. From the magnetic long wavelength map in Figure 3 it can be seen that the long wavelength anomaly maxima correlate remarkably well with ore mineralizations; i.e. rocks hosting ores (serpentinites + magnetite and / or black schists + pyrrhotite).

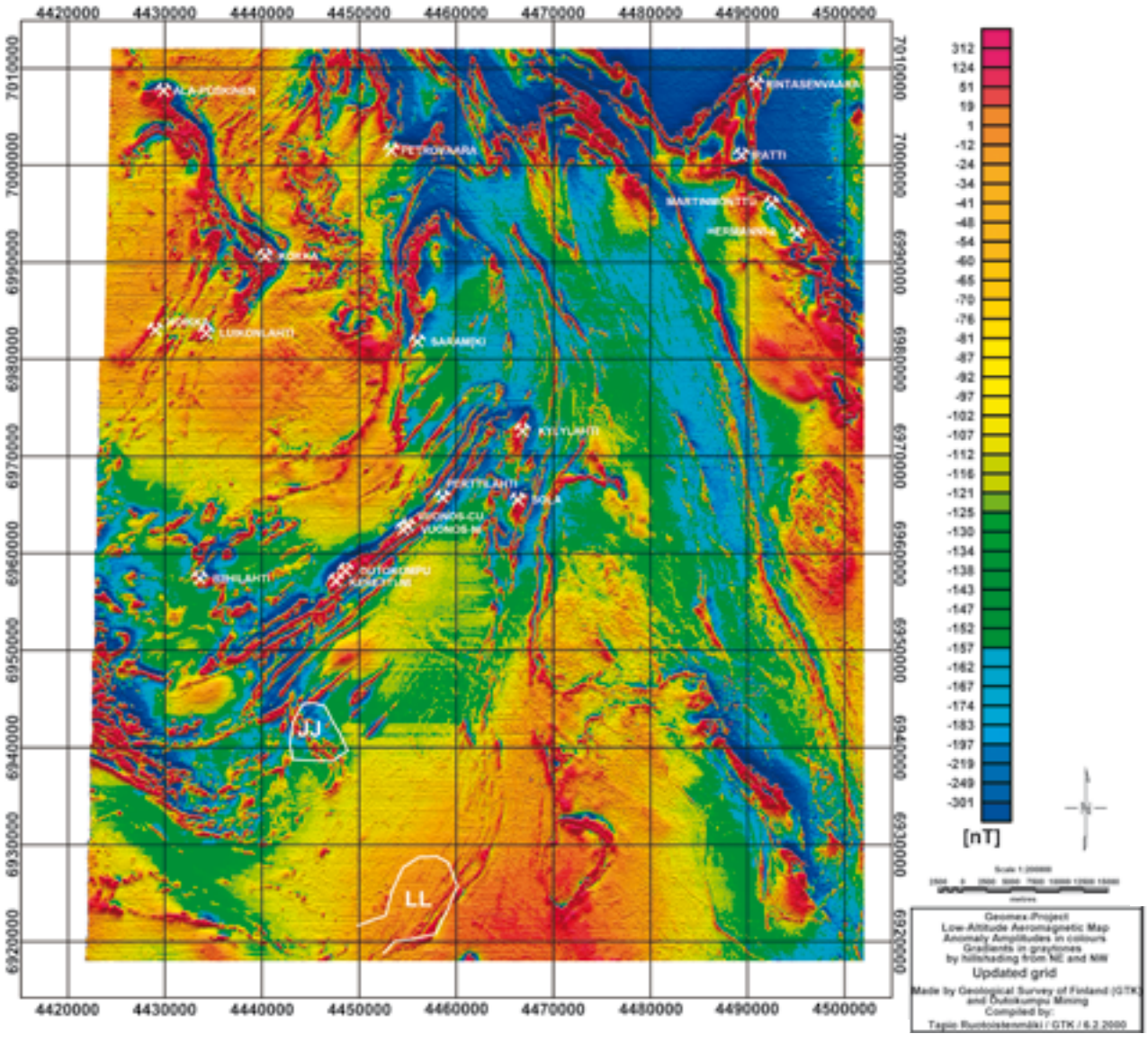

Figure 2. Magnetic high-resolution map of the study area. The map has been compiled from data measured by the Geological Survey of Finland. The hammers show the location of the most important mines and ore showings in the area. The anomalies JJ (Juojärvi) and LL (Leppälahti) will be considered later.

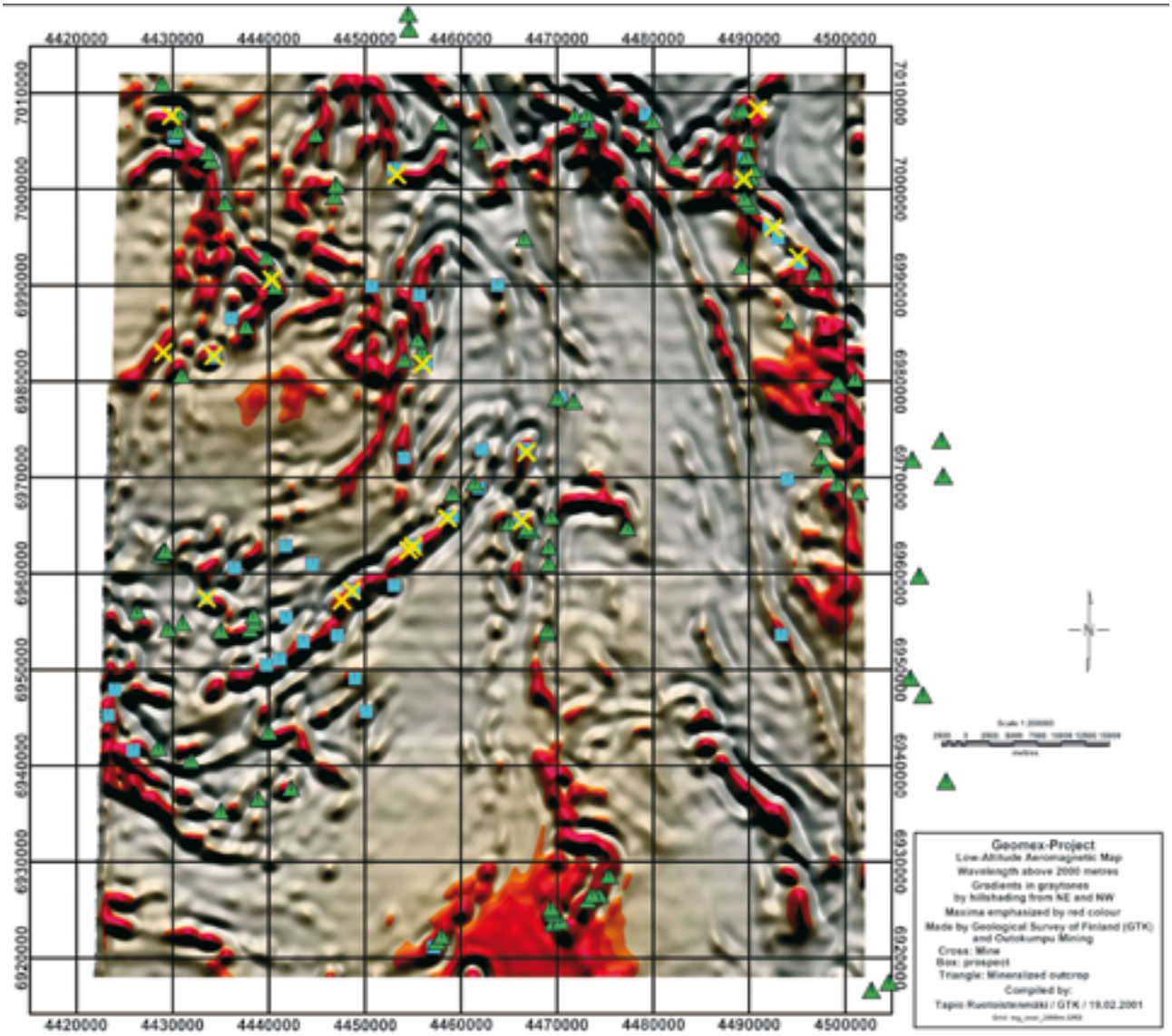

Figure 3. Filtered magnetic map. Wavelengths above 2000 m. The high amplitude anomalies have been emphasized with red colour. Crosses, boxes and triangles respectively depict the location of mines, prospects and mineralized outcrops in the study area.

Gravity map

The gravity map of the study area is shown in Figure 4. The map has been compiled from regional scale data measured by the Geodetic Survey of Finland (with a grid of ca. 5000 x 5000 metres) and local scale data by GTK (ca 500 x 500 metres) and Outokumpu Mining Oy (ca 2000 x 2000 metres; central part of the map). The boundaries between the local and regional scale data sets are visible as discontinuities in anomaly amplitudes and frequencies. The ridge due to the Outokumpu zone (OZ) is bordered by gravity minima due to Maarianvaara granite (MV) and Sotkuma Archaean gneiss dome (ST).

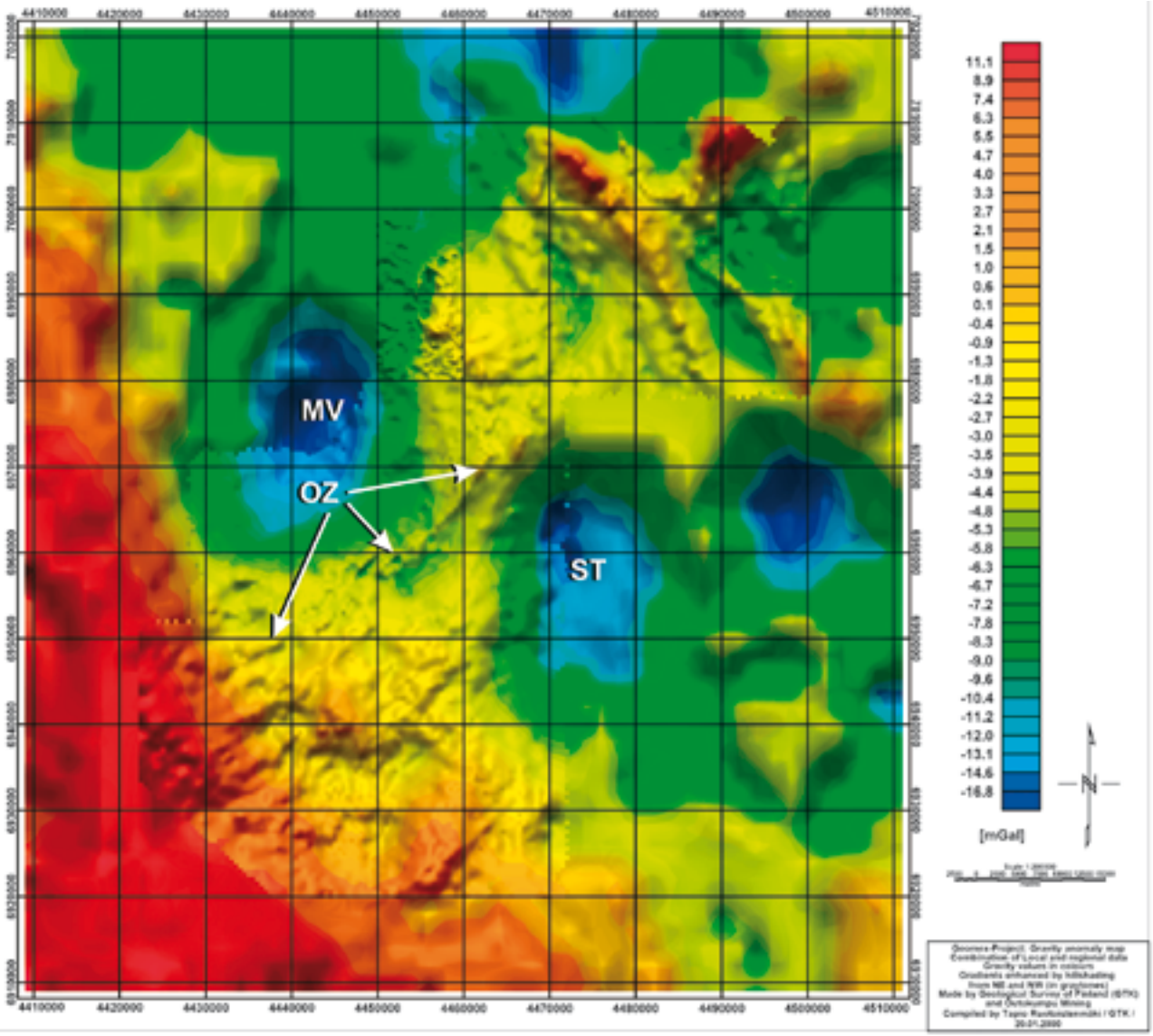

Figure 4. Gravity map of the study area. The map has been compiled from data measured by the Geological Survey of Finland and Outokumpu Mining Oy. MV = Maarianvaara granite minimum, ST = Sotkuma gneiss dome minimum, OZ = Outokumpu zone maximum.

Electromagnetic maps

The continuity of the magnetic anomaly zones in the Geomex area shown in Figure 2 is most evident on the low-altitude electromagnetic maps, reflecting electric conductivity variations in the bedrock and soil cover. The real (in-phase) component map in Figure 5 is especially informative.

From Figure 5 it can be seen, for example, that the linear Outokumpu anomaly zone (OZ) is cut by a sinistral fault (C) and further south by the sinuous Juojärvi anomaly zone (JZ). In the NW part of the Outokumpu zone, the doubly plunging Miihkali basin (MB) can be explained as an interference structure caused by two crossing synforms. The Outokumpu and Miihkali anomaly zones are both surrounded by the very long and coherent Haaralaniemi anomaly (HA), which can be interpreted to represent the edges of a relatively continuous thrust surface below the Outokumpu and Miihkali anomaly areas. The Sotkuma (ST) and Liperinsalo (LP) basement 'windows' are seen to protrude through the younger metasediments, possibly also representing interference structures (see interpretation in Figure 23). The quadrature (out of phase) component electromagnetic map in Figure 6 emphasizes less conductive local scale anomalies that partly mask the highly conductive regional anomalies shown in Figure 5.

By combining the graytone magnetic map, hillshaded from NE and NW and the electromagnetic

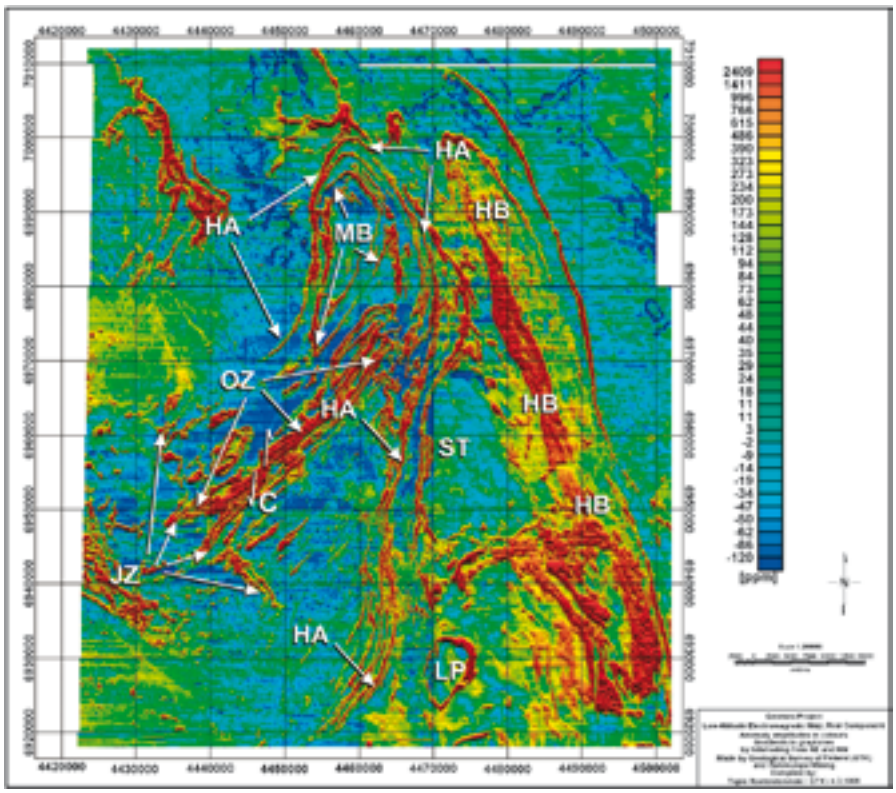

Figure 5. Electromagnetic real (in-phase) component map of the study area. The map has been compiled from data measured by the Geological Survey of Finland. OZ = Outokumpu anomaly zone, C = shear zone, JZ = Juojärvi anomaly, MB = Miihkali 'basin', HA = Haaralanniemi anomaly, HB = Höytiäinen basin, LP = Liperinsalo 'window', ST = Sotkuma basement 'window'.

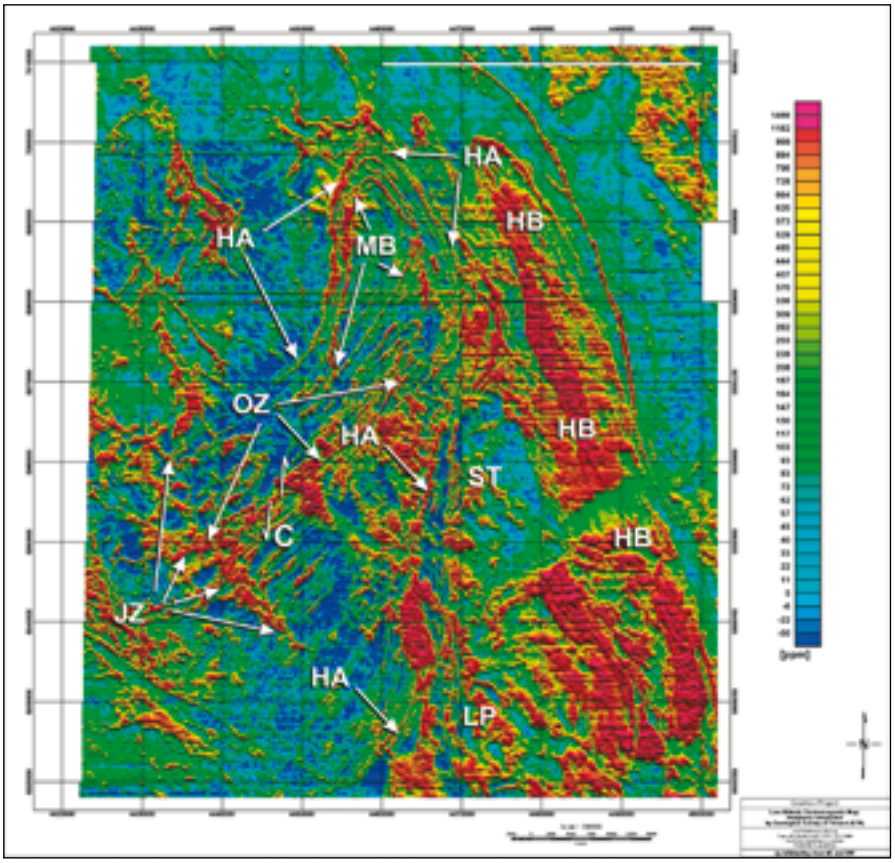

Figure 6. Electromagnetic quadrature (out-of-phase) component map of the study area. The map has been compiled from data by the Geological Survey of Finland. Abbreviations are the same as in Figure 5.

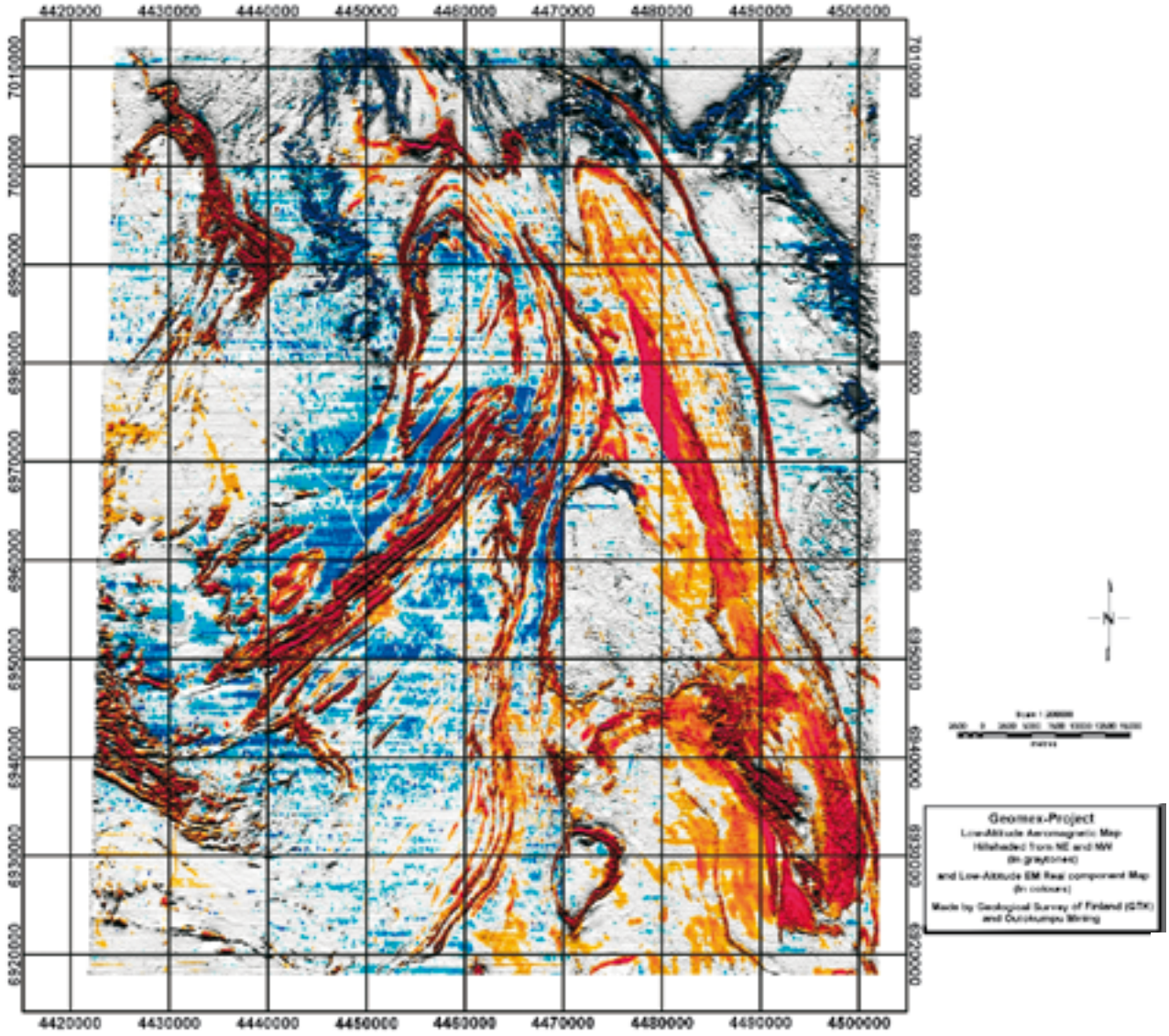

Figure 7. Combined magnetic and electromagnetic real components. The magnetic anomalies are depicted in graytones hillshaded from NE and NW. The electromagnetic in-phase maxima are given in red and minima with blue.

real component map (in colour), pyrrhotite bearing electrically conductive black schists (magnetic high and EM real high (red) in Figure 7) can be separated from magnetite bearing poorly conductive rocks (magnetic high and EM real low (blue)). For the principles underlying this method, see Peltoniemi (1982 and references therein). From the combination map it can be seen that for most of the Outokumpu, Miihkali, Juojärvi, Höytiäinen and Haaralanniemi anomalies, the main magnetic source is pyrrhotite. Most of the magnetite-dominant anomaly zones are on the NE parts of the map and relate to ca. 2.2 Ga layered intrusions (Asko Kontinen, GTK, 2005, pers. comm.).

Radiometric maps

In general, the radiometric data are noisy and strongly dampened by overburden, especially in wetland areas; over lakes radiometric anomalies cannot be detected at all. Therefore, single component maps of potassium, uranium, thorium, as well as total radiation in areas of thick overburden are in general not very useful. Thus, various versions of ternary and ratio maps are preferred, as demonstrated in maps below.

The U-K-Th ternary map of the study area is shown in Figure 8, with some overlays adopted from Figure 1. It can be seen from this map that the Outokumpu nappe and the NW and NE corners of the study area are dominated by the U – Th -combination. In the

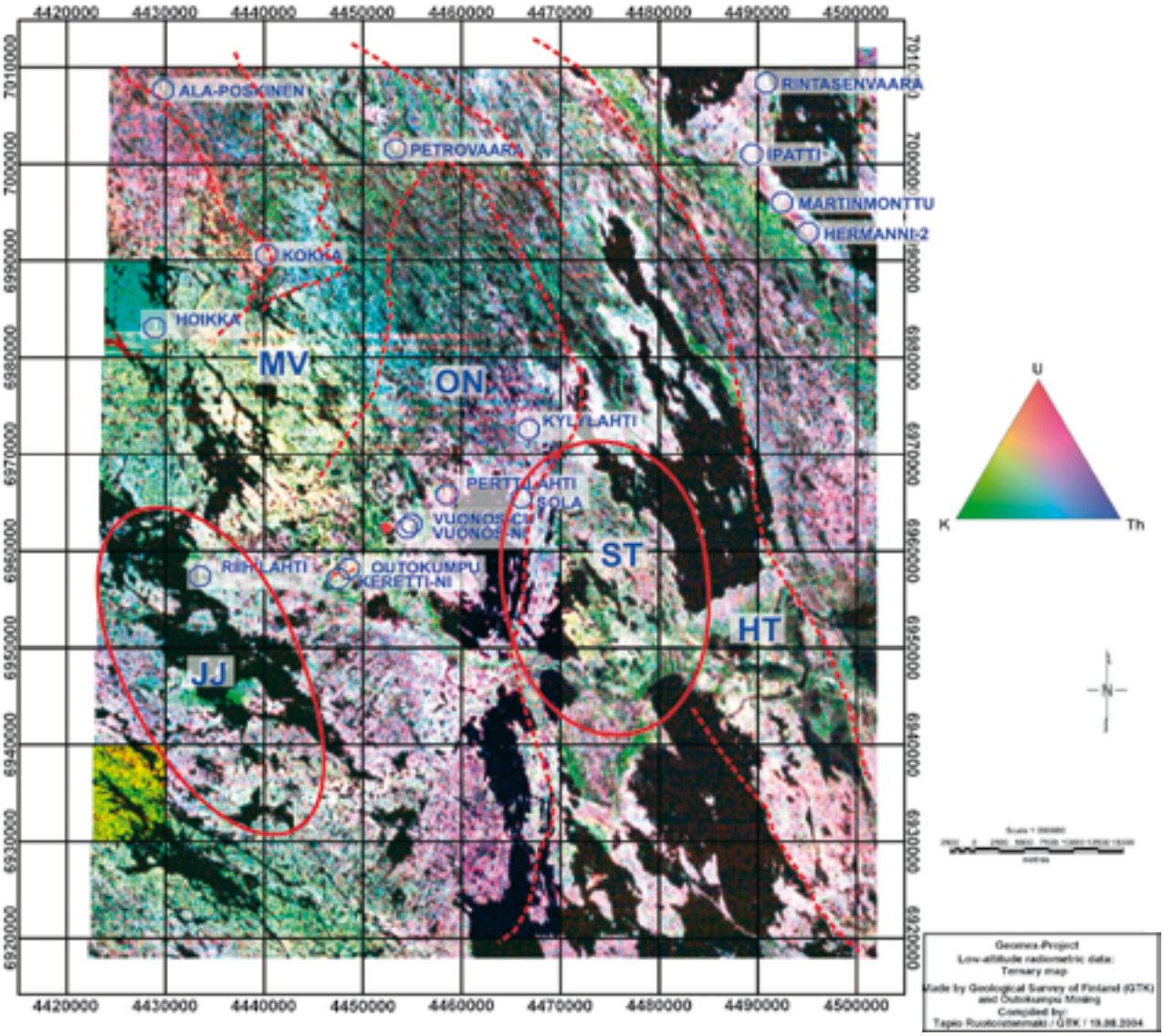

Figure 8. Radiometric ternary map of the study area. K = potassium, Th = thorium, U = uranium components. The overprints have been partly adopted from Figure 1. Solid red circles: Areas of Archaean basement windows. Dashed lines: Svecofennian deformation zones. Small blue circles: Mines. MV: Maarianvaara granitoid, ON: Outokumpu Nappe, ST: Archaean Sotkuma dome, JJ: Archaean Juojärvi dome area, HT: Höytiäinen block. The black areas are mainly lakes.

Maarianvaara granitoid area potassium is dominant. In the Juojärvi and Sotkuma basement areas potassium radiation is also locally higher. In the SE corner of the Höytiäinen area the thorium component is less pronounced.

It is also interesting to note the relatively high uranium peaks (red dots) in the Keretti-Outokumpu -Vuonos mine areas, probably due to waste rock piles from the mines. The possible reasons for increase in U in ore potential areas is considered below.

Ratios of radiometric components

Variation in the absolute intensity of gamma radiation is not only dependent on source rock minerology, but also on the nature and thickness of the material covering the bedrock, in particular on its water content. This effect has been suppressed by using ratios of various radiometric elements. For example the U/Th -ratio may indicate variations in the oxidation state of hydrothermal processes in rocks and ore bearing fluids (e.g. Kivekäs, 1974).

The U/Th-ratio of cumulative frequencies of all grid points in the study area (1 962 505 points, background values eliminated) and interpolated U/Th-ratios on coordinate points from 11 mines, 30 prospects and 71 mineralized outcrops are given in Figure 9.

The curves in Figure 9 indicate that ca. 10% of all grid points have U/Th-ratios above 0.4 in the survey area. However, ca. 35 % of mine points have U/Th-

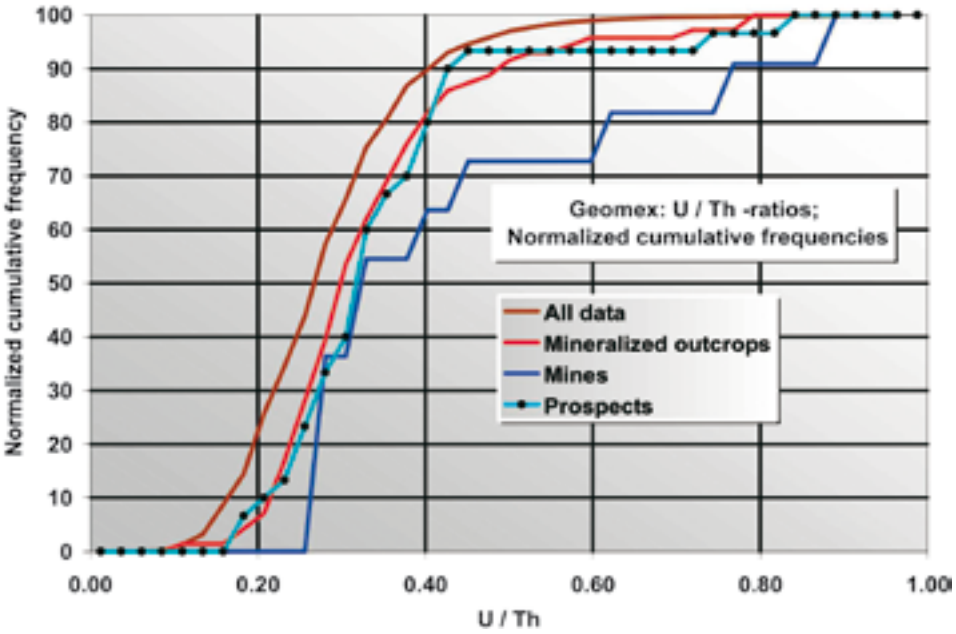

Figure 9. Cumulative frequencies of U/Th ratios in the radiometric data of the study area.

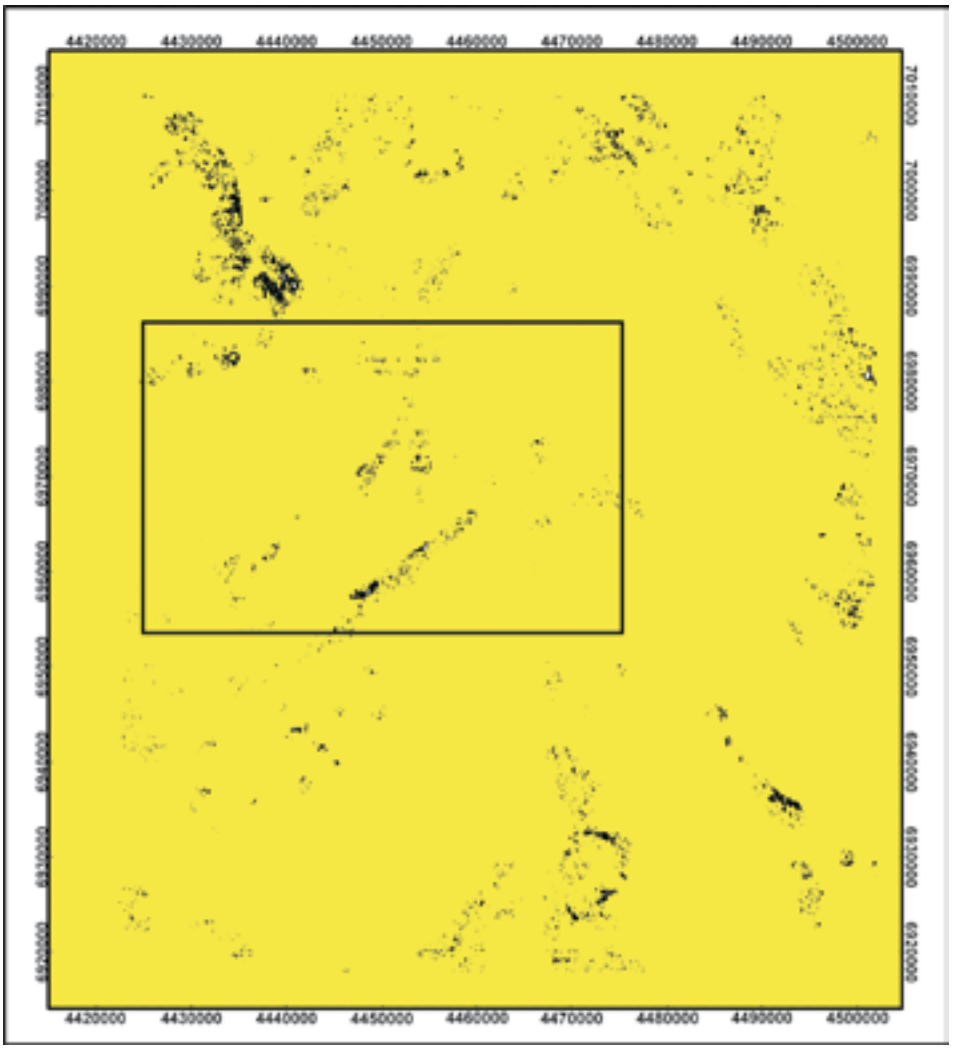

Figure 10. Combined U/Th and long wavelength magnetic map of the study area. The black dots show localizations where U/Th is above 0.4 and magnetic long wavelength anomalies above 4 nT. The background is in yellow for clarity. The framed area is shown in more detail in Figure 11.

Figure 11. Combined U/Th and long wavelength magnetic anomaly map of the central part of the study area. The coloured dots show areas where U/Th is above 0.4 and magnetic long wavelength anomalies above 4 (red values in Figure 3). The major mines are shown with crossed hammers.

ratios above 0.4. From the figure it becomes evident that many of the prospects and mineralized outcrops have anomalously high U/Th-ratios. Airo and Loukola-Ruskeeniemi (2004) have also noted that the Outokumpu-type deposits are spatially associated with black schists with enhanced U and relatively low Th in the mineralized zones, and often low K values in airborne gamma-ray data.

Figure 10 depicts localizations where both, U/Th values and magnetic long wavelength values are high. The framed area in the central part of the map is shown in more detail in Figure 11. From these figures, it can be seen that the anomalies correlate well with the locations of mines and especially, the main Outokumpu zone from Keretti to Perttilahti. Besides the major Outokumpu ore zone there are also other distinct and large anomalous zones revealed by high U/Th and long wavelength magnetic anomalies.

PETROPHYSICAL PROPERTIES OF ROCK SAMPLES

GTK data base

The petrophysical laboratory of the Geological Survey of Finland (GTK) has made ca. 2100 petrophysical measurements of surface rock samples in the Geomex area. The parameters considered below are susceptibility and density and a susceptibility-density diagram for the GTK samples is shown in Figure 12. The density and susceptibility values of the peaks in the diagram are given in Table 1.

The petrophysical data were further classified by the parameter ‘distance’ related to a normalized distance of a sample from the peaks in the diagram. The smaller the value, the closer the sample is to the peak; i.e. the more representative the sample is to the class defined by the susceptibility-density value of the peak. Table 2 gives the ten closest samples for each class (except class 8, which includes only seven samples).

From the Table 2 it can be seen that in most classes the variations in rock type of the closest samples are small and thus it can be concluded that the method is relatively well in selecting representative samples for various petrophysical rock types in the area. However, in class three the rock types vary in an irregular manner, even though the peak in the diagram in Figure 12 is relative high and sharp. For such classes one must search for other explanations independent of rock types, such as degree of metamorphism.

Class 1: Class 1 samples are mainly mica gneisses, which are the dominant rock type in the whole area. Their density is ‘felsic’ (i.e. close to granite-grano-

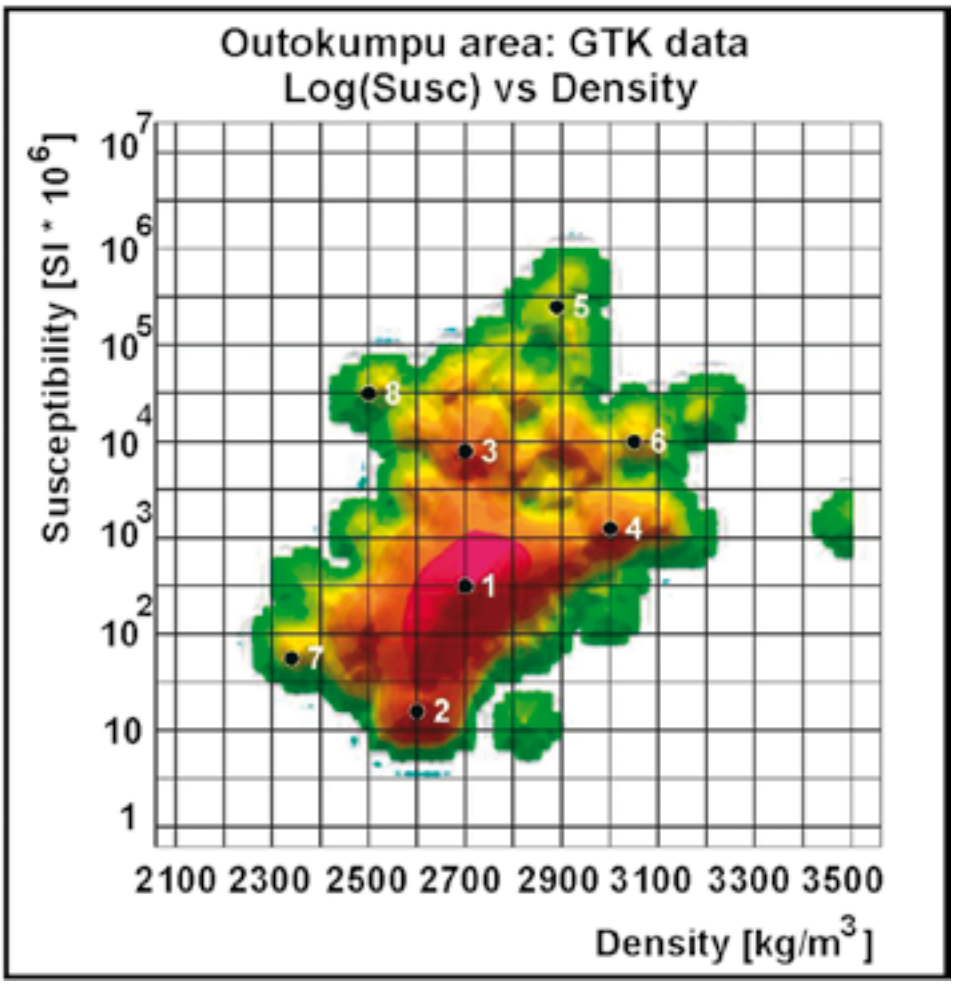

Figure 12. Susceptibility – density diagram of GTK samples from the Geomex study area. The amplitude of the diagram is proportional to the number of samples in its close surroundings. The data have been classified visually by selecting the most prominent peaks. The black dots depict the location of the peaks, numbered from 1 to 8.

Table 1. Density and susceptibility values related to the peaks in diagram in Figure 12.

Peak number	Density [kg/m^3]	Susceptibility [*10^6 SI]	Log(Susceptibility [*10^6 SI])
1	2700	316.2	2.5
2	2600	15.8	1.2
3	2700	7943.2	3.9
4	3000	1258.9	3.1
5	2890	251188.6	5.4
6	3050	10000	4
7	2340	56.2	1.75
8	2500	31622.7	4.5

diorite density) and susceptibility is low and paramagnetic.

Class 2: Class 2 consists of even less dense and non-magnetic rocks, mainly tonalites. However, the peak density of ca. 2600 kg/m^3 is surprisingly low for ordinary tonalites. For example the average of densities of ca. 1600 tonalite samples in the GTK petrophysical database is ca. 2707 kg/m^3. The low-density tonalities are mainly located SW of the Juojärvi zone (see Figure 13) and their low density could possibly be associated with tectonic and metasomatic alteration processes during the emplacement of the Outokumpu nappe and later folding processes. These samples clearly cannot explain the high gravity anomalies SW from the Juojärvi zone, which thus must originate from deeper, higher density anomaly sources.

Class 3: The samples in class 3 have 'felsic' densities and ferrimagnetic susceptibilities. The rock types are variable and no simple rock group can be defined, though the peak in Figure 12 is high and sharp.

Classes 4 and 5: The samples in classes 4 and 5 mainly comprise mafic metavolcanic rocks and metadiabases. The samples in class 5 are less dense but strongly ferrimagnetic; iron is thus concentrated more in magnetite and less in silicates compared to class 4, where the samples are denser but less ferrimagnetic.

Table 2. The closest samples of each class to the peak values of the samples in GTK data base.

Rock Type Name	Class	Distance	Density [kg/m^3]	Susceptibility [*10^6 SI]	Log(Susceptibility) [*10^6 SI]
mica gneiss	1	0.07	2699	320	2.51
mica gneiss	1	0.10	2698	316	2.50
mica gneiss	1	0.12	2699	324	2.51
mica gneiss	1	0.16	2703	312	2.49
garnet mica gneiss	1	0.19	2697	307	2.49
mica gneiss	1	0.21	2703	327	2.51
mica gneiss	1	0.21	2696	322	2.51
mica gneiss	1	0.22	2701	301	2.48
mica gneiss	1	0.22	2699	301	2.48
mica gneiss	1	0.22	2696	309	2.49
medium grained tonalite	2	0.04	2600	16	1.20
medium grained tonalite	2	0.28	2597	15	1.18
medium grained granodiorite	2	0.30	2599	17	1.23
medium grained tonalite	2	0.40	2608	16	1.20
medium grained tonalite	2	0.53	2599	14	1.15
medium grained tonalite	2	0.59	2588	16	1.20
coarse-grained tonalite	2	0.62	2594	18	1.26
granodioritic pegmatite	2	0.72	2610	14	1.15
coarse-grained tonalite	2	0.84	2584	17	1.23
fine grained tonalite	2	0.98	2588	19	1.28
quartz-feldspar gneiss	3	0.16	2697	8079	3.91
talc schist	3	0.32	2694	7708	3.89
veined gneiss	3	0.54	2689	7935	3.90
soapstone	3	0.59	2693	7101	3.85
conglomerate / etc	3	0.99	2680	7960	3.90
conglomerate / etc	3	1.04	2679	8110	3.91
veined gneiss	3	1.05	2712	9729	3.99
serpentinite	3	1.23	2725	8021	3.90
conglomerate / etc	3	1.32	2684	6210	3.79
mica gneiss	3	1.36	2719	10014	4.00
skarn	4	0.50	3000	1120	3.05
metadiabase	4	0.61	3002	1450	3.16
mica gneiss	4	0.62	3011	1171	3.07
amphibolite	4	0.67	3000	1077	3.03
mica gneiss	4	1.08	2979	1176	3.07
metadiabase	4	1.14	2977	1302	3.11
amphibolite	4	1.24	2977	1415	3.15
mica gneiss	4	1.30	3007	940	2.97
amphibolite	4	1.42	3020	990	3.00
amphibolite	4	1.44	3002	900	2.95
greenstone / greenschist	5	1.45	2866	206644	5.32
metadiabase	5	2.33	2843	238477	5.38
diabase / dolerite	5	2.35	2900	429500	5.63
diabase / dolerite	5	2.72	2921	425440	5.63
amphibolite	5	2.87	2910	133690	5.13
soapstone	5	3.47	2918	119274	5.08
diabase / dolerite	5	5.18	2814	109020	5.04
soapstone	5	6.70	2911	53519	4.73
serpentinite	5	7.33	2927	47812	4.68
diorite	5	8.11	2756	83504	4.92
serpentinite	6	0.17	3051	9637	3.98
serpentinite	6	1.52	3071	12984	4.11
sialic gneiss	6	1.54	3070	7574	3.88
serpentinite	6	1.87	3047	15451	4.19
serpentinite	6	2.43	3001	10696	4.03
greenstone / greenschist	6	2.84	3091	6277	3.80
serpentinite	6	3.09	2998	6668	3.82
serpentinite	6	5.15	2956	5903	3.77
serpentinite	6	5.32	2961	4942	3.69
felsic gneiss	6	5.44	2942	7660	3.88
black schist	7	0.58	2346	50	1.70
black schist	7	0.61	2333	50	1.70
graphite schist	7	1.31	2314	60	1.78
graphite schist	7	2.04	2312	80	1.90
veined gneiss	7	2.45	2388	65	1.81
veined gneiss	7	3.76	2402	94	1.97

Continue

Table 2. Continues

Rock Type Name	Class	Distance	Density [kg/m^3]	Susceptibility [*10^6 SI]	Log(Susceptibility) [*10^6 SI]
mica gneiss	7	4.49	2431	60	1.78
mica gneiss	7	4.62	2429	40	1.60
black schist	7	5.22	2403	150	2.18
black schist	7	5.61	2440	30	1.48
serpentinite	8	1.01	2518	35370	4.55
serpentinite	8	1.17	2520	36710	4.56
serpentinite	8	1.44	2474	27170	4.43
serpentinite	8	4.79	2558	12886	4.11
serpentinite	8	5.00	2581	15626	4.19
medium grained granite	8	5.62	2607	20080	4.30
olivine rock	8	6.01	2570	10012	4.00

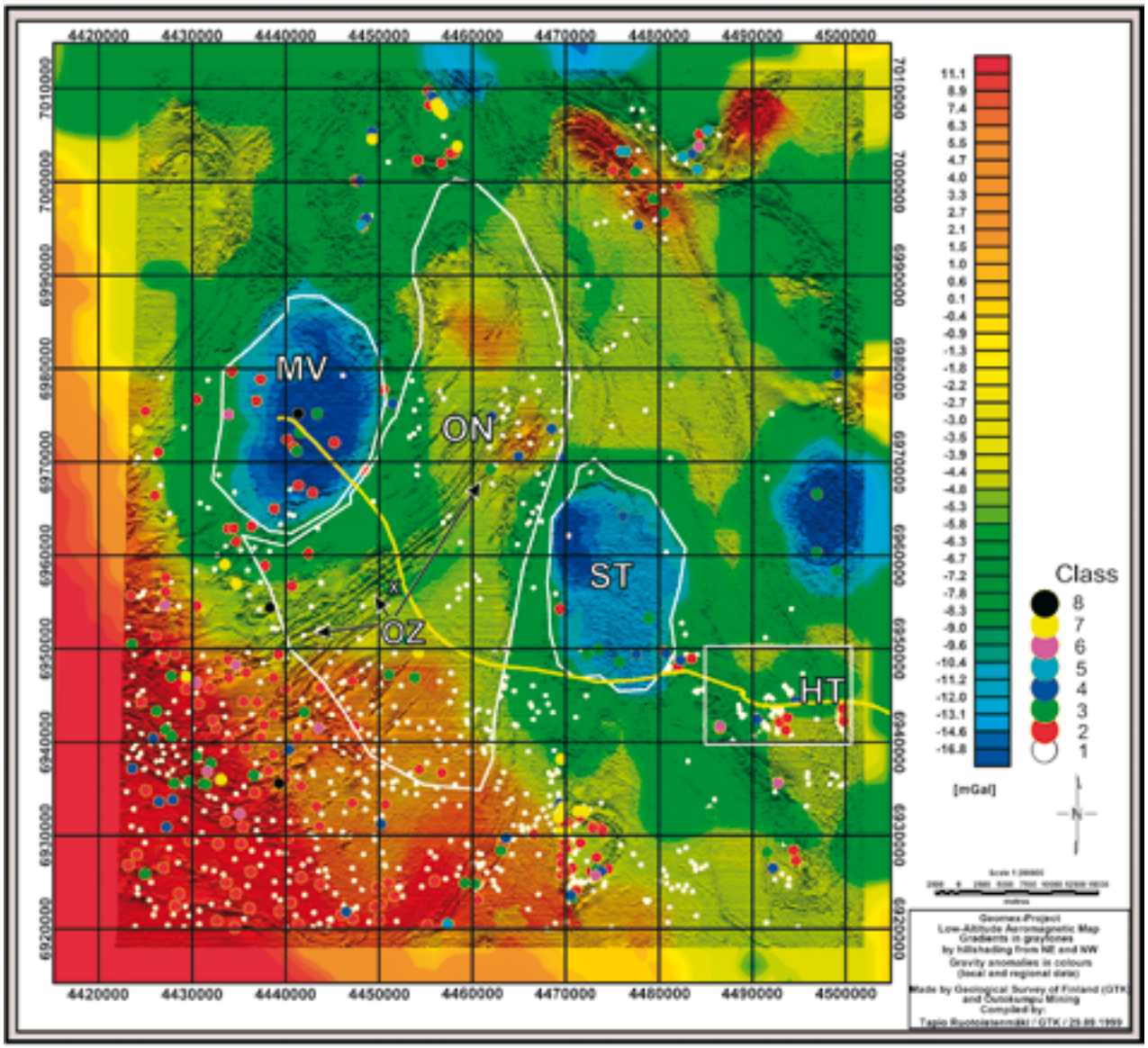

Figure 13. Sample locations on a combination of gravity maps (in colours) and magnetic maps (graytones, hillshaded from NE and NW). Symbols refer to classes 1 – 8 in Table 1. Samples in subareas bordered by white lines are considered later in text. MV = Maarianvaara granite minimum, ST = Sotkuma gneiss dome minimum, ON = Outokumpu nappe area, HT = samples from the Höytiäinen area. OZ = trend of the ore potential Outokumpu anomaly zone. The yellow line shows the trend of the NW segment of the FIRE-3 deep seismic reflection profile (Kukkonen et al., 2006) and the cross (X) on the SE edge of the Outokumpu zone shows the location of the drill hole of the Outokumpu Deep Drilling Project carried out by GTK (Kukkonen, 2006), both of which are referred to later in text.

Classes 6 and 8: The samples in classes 6 and 8 mainly comprise different types of serpentinites. The samples in class 8 are less dense but more strongly magnetized, probably chrysotile serpentinites. The densities of samples in class 6 are high, exceeding typical densities of serpentinites (including antigorites). Thus they are probably rich in iron sulfides or contain e.g. carbonates ± talc (see also Lehtonen (1981)).

Class 7: The samples in this class are mainly black schists and graphite-bearing mica schists. Their densities are very low and susceptibility is paramagnetic. Thus, they are shown as minima in gravity and magnetic maps.

The locations of all GTK samples are shown as coloured dots according to their class in Figure 13. It is interesting to note that the low-density and low susceptibility class number 2 (tonalites) is concentrated towards the SW corner of the area where the gravity anomalies are elevated, which relates to higher density sources below the outcropping surface rocks.

Outokumpu drill hole data base

The petrophysical data provided by Outokumpu Mining Oy for the Geomex project comprised 9584 measurements of drill core samples. In general, it can be assumed that the sampled drill holes were located in anomalous zones where economic sulfide mineralizations were expected to occur. In contrast, the GTK petrophysical samples were intended to be representative of the general bedrock variations in the area. Thus, there should be far less bias in the GTK data set. The susceptibility-density diagram of the Outokumpu Mining samples is shown in Figure 14. The density and susceptibility values related to the peaks of the diagram are given in Table 3.

Table 3. Density and susceptibility values related to the peaks in the diagram in Figure 14

Peak Number	Density [kg/m^3]	Susceptibility [*10^6 SI]	Log(Susceptibility [*10^6 SI])
1	2765	125.9	2.1
2	2900	158.5	2.2
3	2540	5011.9	3.7
4	2765	631.0	2.8
5	2775	19952.6	4.3
6	2490	100.0	2
7	3250	316.2	2.5
8	3000	10.0	1
9	3300	12589.3	4.1
10	2600	10.0	1

When comparing the diagrams in Figures 12 and 14, it is evident that they represent totally different data sets, the distributions in drill hole data being much wider. Table 2 presents the ten closest samples of each class.

Classes 1 and **4** represent various metasedimentary rocks (mica schists, black schists etc) having 'felsic' densities and low magnetic susceptibilities. In class 4 susceptibility is relatively high and paramagnetic, reflecting high iron contents in silicates. From Figure 16 it can be seen that class 4 is the major class of black schists.

Classes 2, **7** and **8** comprise mainly high density and low susceptibility skarns. In class 7 the density is so high that the samples must represent ore-grade sulfide mineralizations, which becomes evident from Figure 15. In samples of the lower density classes 2 and 8, the sulfide mineral potential is smaller.

Classes 3, 5 and **6** mainly include serpentinites. Classes 3 and 6 have low density, class 3 being ferri- and class 6 paramagnetic. The rock types in class 5 are more varied and have the highest densities and susceptibilities. These classes are good examples of ability of the method to classify rocks by their petrophysical parameter combinations.

Class 9 consists of high density and susceptibility ultramafic rocks or sulfide bearing rocks.

Class 10 consists of various type felsic or altered rocks having very low densities and susceptibilities.

The Outokumpu drill hole database also contains information on the ore mineral contents of the measured samples. Thus, it is to some extent also possible to analyze which of the petrophysical classes would have the most ore potential. Figure 15 gives a presentation of the Cu mineralization potential of each class. Using this approach, classes 7 and 2, which mainly represent skarns, have the highest Cu-ore potential. It is interesting to note that both are paramagnetic (and high density) classes. However, from the long wavelength magnetic map in Figure 3 it is evident that the ore mineralizations in the area are embedded within high, long wavelength magnetic anomalies; i.e. the ore mineralizations are locally non-magnetic, but at a regional scale within magnetic environments. Airo and Loukola-Ruskeenniemi (2004) also observed that locally reduced magnetization is characteristic of Outokumpu type mineralizations in eastern Finland.

Figure 16 gives an example of the classification of rock type (black schists) based on density – susceptibility -classes. Black schists fall mainly in classes 4, 2 and 1 which all fall within the main paramagnetic population in Figure 14. However, their densities vary significantly, between ca. 2760 – 2900 kg/m^3.

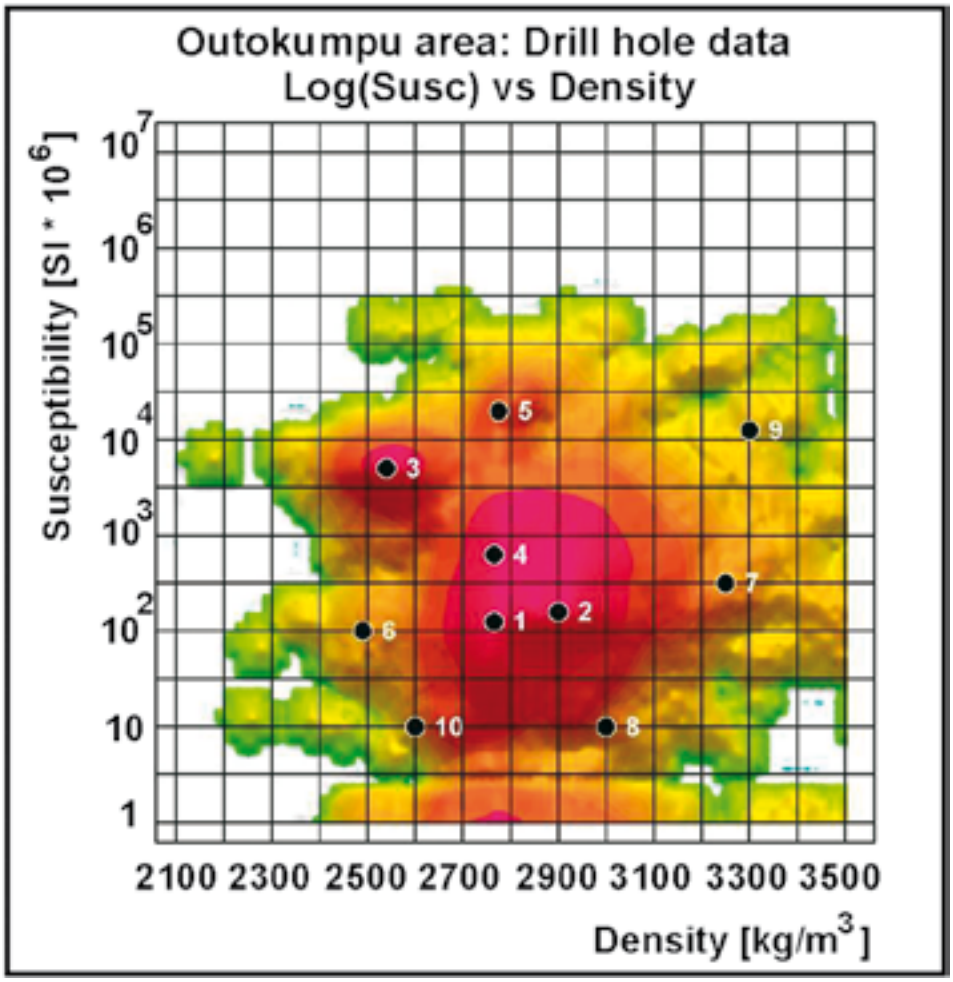

Figure 14. Susceptibility-density diagram for the Outokumpu petrophysical database.

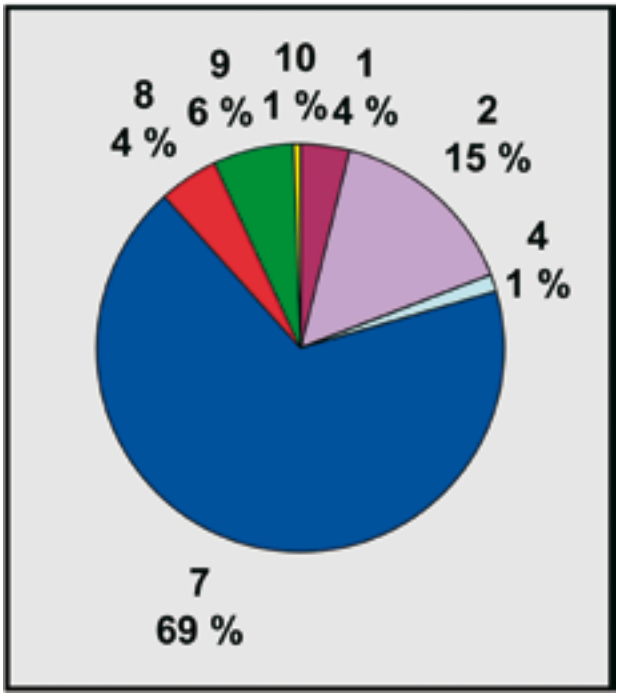

Figure 15. Outokumpu drillhole petrophysical data: Cu-potential classes.

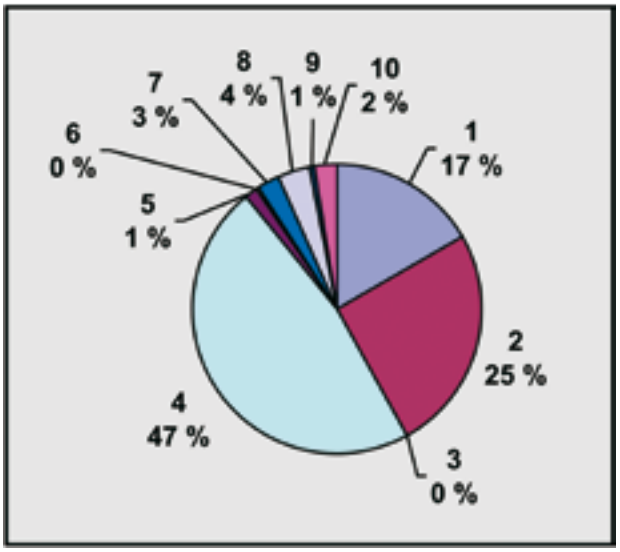

Figure 16. Outokumpu drillhole petrophysical data: Black schist classification by density and susceptibility.

Table 4. The closest samples for each class to the peak values of the samples in the Outokumpu data base (the rocknames are uncertain field names).

Rockname	Class	Distance	Density [kg/m³]	Susceptibility [*10⁶ SI]	Log (Susceptibility) [*10⁶ SI]
mica-tremolite skarn	1	0.25	2760	126	2.10
mica schist	1	0.25	2760	125	2.10
quartzite skarn	1	0.25	2760	127	2.10
black schist	1	0.25	2770	128	2.11
sericite schist	1	0.26	2760	128	2.11
mica gneiss	1	0.26	2770	124	2.09
mica schist	1	0.26	2770	129	2.11
mica gneiss	1	0.27	2770	123	2.09
mica schist	1	0.28	2770	122	2.09
chlorite-carbonate-biotite gneiss	1	0.29	2760	122	2.09
talc-tremolite rock	2	0.01	2900	159	2.20
chlorite schist + tremolite skarn	2	0.04	2900	160	2.20
black schist	2	0.17	2900	165	2.22
quartzite skarn	2	0.17	2900	165	2.22
talc-carbonate rock	2	0.22	2900	167	2.22
tremolite skarn	2	0.27	2900	169	2.23
talc-carbonate rock	2	0.29	2900	148	2.17
talc schist	2	0.29	2900	148	2.17
skarn quartz rock	2	0.42	2900	144	2.16
talc schist	2	0.49	2890	158	2.20
serpentinite	3	0.01	2540	5021	3.70
serpentinite	3	0.02	2540	4993	3.70
serpentinite	3	0.06	2540	4946	3.69
serpentinite	3	0.07	2540	5099	3.71
serpentinite	3	0.13	2540	5171	3.71
serpentinite	3	0.17	2540	5212	3.72
serpentinite	3	0.23	2540	5292	3.72
serpentinite	3	0.28	2540	4693	3.67
serpentinite	3	0.32	2540	4647	3.67
serpentinite	3	0.49	2530	5027	3.70
quartzite	4	0.25	2760	630	2.80
mica schist+ black schist	4	0.25	2760	635	2.80
black schist	4	0.25	2760	626	2.80
quartzite	4	0.25	2760	637	2.80
gneiss, skarn (?)	4	0.25	2760	623	2.79
serpentinite	4	0.26	2760	641	2.81
mica schist	4	0.28	2770	649	2.81
graphitic gneiss	4	0.28	2770	652	2.81
black schist	4	0.28	2770	611	2.79
mica schist	4	0.29	2770	654	2.82
soapstone, talc rock	5	0.26	2770	20309	4.31
serpentinite	5	0.28	2780	20576	4.31
serpentinite, magnetite-bearing	5	0.32	2770	19040	4.28
carbonate serpentinite	5	0.39	2780	18614	4.27
soapstone	5	0.44	2780	21705	4.34
carbonate serpentinite	5	0.47	2780	18188	4.26
carbonate serpentinite	5	0.54	2780	22349	4.35
carbonate serpentinite	5	0.58	2780	17670	4.25
magnetite-bearing soapstone	5	0.64	2780	17389	4.24
serpentinite	5	0.71	2770	17083	4.23
serpentinite	6	0.26	2490	106	2.03
serpentinite	6	0.34	2490	92	1.97
serpentinite	6	0.92	2490	81	1.91
serpentinite	6	0.98	2500	122	2.09
serpentinite	6	1.14	2470	87	1.94
serpentinite	6	1.20	2470	117	2.07
serpentinite	6	1.31	2470	122	2.09
quartz-carbonate-tremolite skarn	6	1.65	2520	119	2.07
serpentinite	6	1.68	2490	148	2.17
serpentinite	6	2.09	2470	154	2.19
skarn	7	0.64	3240	287	2.46
skarn + pyrite + iron sulfides (?)	7	0.71	3260	280	2.45
chlorite-cummingtonite-antophyllite (-rock?)	7	0.83	3240	270	2.43
skarn	7	0.85	3240	269	2.43
tremolite-carbonate skarn	7	0.90	3240	265	2.42
tremolite skarn	7	1.05	3270	291	2.46
pyritic ore	7	1.15	3230	363	2.56
skartn quartz rock	7	1.32	3250	430	2.63
black schist	7	1.43	3240	231	2.36
pyrrhotite-rich skarn	7	1.55	3220	285	2.45
actinolite skarn + chlorite schist	8	0.49	2990	10	1.00
tremolite skarn	8	0.57	3010	11	1.03
quartzite skarn	8	0.58	3010	9	0.97
tremolite skarn	8	0.71	3000	12	1.07
actinolite skarn	8	0.82	2990	12	1.07
tremolite skarn	8	0.96	3000	8	0.90
tremolite skarn	8	0.99	2980	10	1.00
dolomite	8	1.07	2990	8	0.90
skarn	8	1.26	2980	12	1.08
dolomite + talc schist	8	1.33	2990	8	0.88
serpentinite	9	0.50	3290	12760	4.11
metaperidotite	9	0.63	3290	13773	4.14
carbonate rock+ pyrrhotite ore	9	0.84	3310	10743	4.03
metaperidotite	9	1.53	3280	16568	4.22
metaperidotite	9	2.20	3330	18399	4.26
metaperidotite	9	2.50	3350	13833	4.14
metaperidotite	9	3.46	3280	5799	3.76
metaperidotite	9	3.71	3300	29969	4.48
pyrrhotite-rich black schist	9	3.92	3350	6182	3.79
metaperidotite	9	4.03	3220	10366	4.02
quartzite breccia	10	0.00	2600	10	1.00
mica schist	10	0.49	2610	10	1.00

Table 4. Continue

Rockname	Class	Distance	Density [kg/m^3]	Susceptibility [*10^6 SI]	Log (Susceptibility) [*10^6 SI]
pyrite + pyrrhotite-bearing					
black schist	10	1.23	2610	13	1.11
quartzite+skarn	10	1.26	2580	12	1.08
serpentinite	10	1.37	2620	8	0.90
quartzite breccia	10	1.48	2630	10	1.00
quartzite breccia	10	1.48	2630	10	1.00
pegmatite	10	1.58	2620	13	1.12
granite pegmatite	10	1.66	2620	14	1.14
mica gneiss	10	1.75	2620	14	1.15

The method used here for petrophysical classification of rock samples differs from those generally used in that it firstly defines the main density-susceptibility combinations in the study area, after which the rocks are classified into those classes. In this way it is possible to get the most characteristic parameter combinations for simultaneous interpretation of gravity and magnetic data. Normally these parameters are averaged separately for the main rock groups, which can sometimes lead to erratic parameter combinations with groups where parameter variations reveal several separate peaks, such as for serpentines (classes 6 and 8 in Table 2, and classes 3, 5 and 6 in Table 4) or mafic metavolcanic rocks (classes 4 and 5 in Table 2).

REGIONAL AND LOCAL SCALE ANALYSIS OF STRUCTURAL GEOMETRY

During the Geomex-project several regional and local scale geophysical interpretations were made using various one- and two -dimensional geophysical data sets. The purpose of the regional modelling was to obtain an overview of structures associated with ore potential zones. The local scale studies (surveys and profiles) were further used for defining drilling sites.

Interpretations at Kylylahti

The Kylylahti serpentinite-talc-carbonate -hosted ore body and its surroundings (see location in Figure 2) were an important target of exploration and study during the project. A detailed magnetic map of the Kylylahti area is shown in Figure 2. The map also shows the location of the cross-section profiles considered below. The geometry of the prominent magnetic anomaly suggests that the Kylylahti area lies within a SW plunging synform.

Geomex project survey at Kylylahti included an

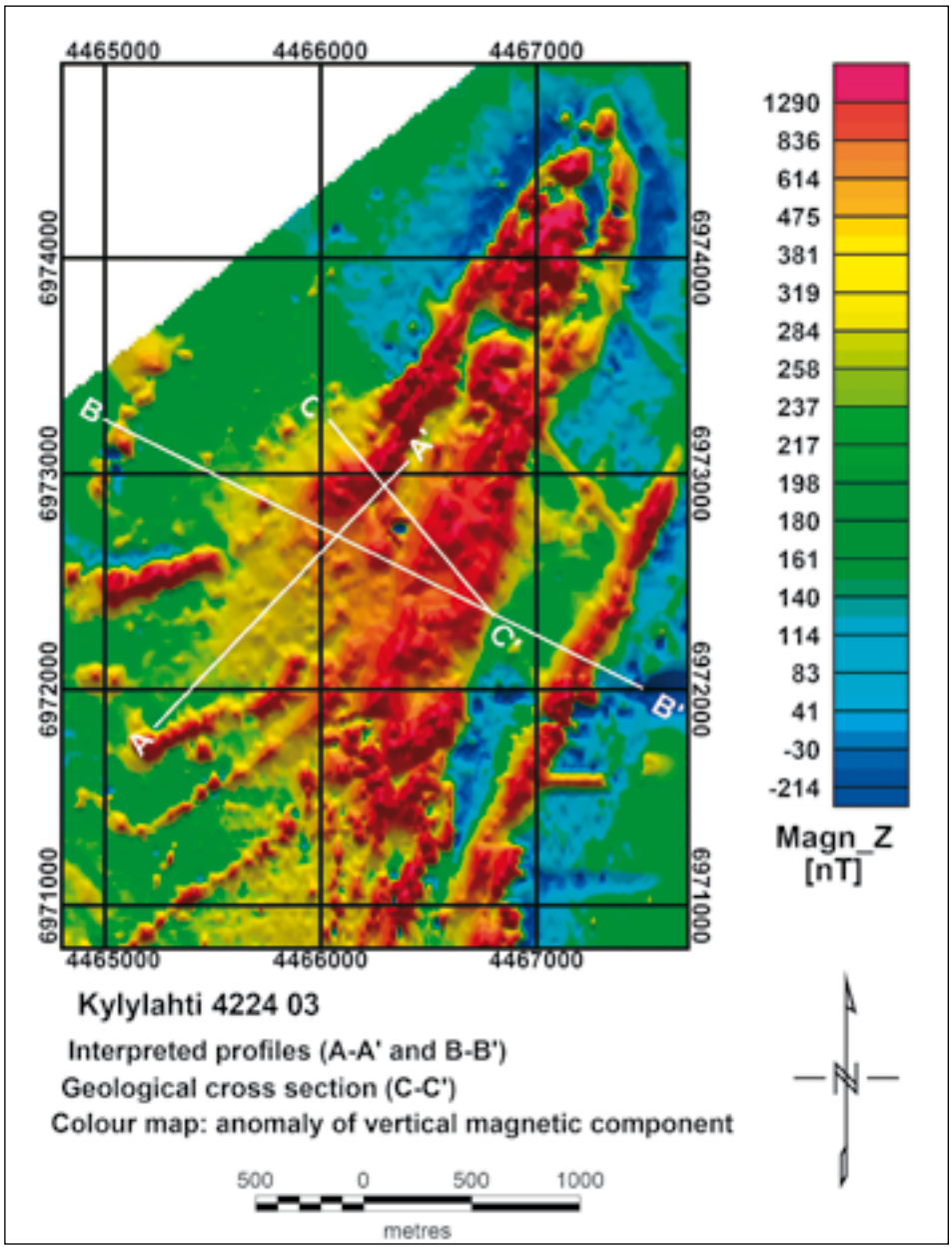

Figure 17. Magnetic map of the Kylylahti area. Profile A – A': Electromagnetic measurements, interpreted in Figure 18. Profile B – B': Gravity and magnetic profiles interpreted in Figure 19. Profile C – C': Lithological cross-section based on drilling results shown in Figure 20.

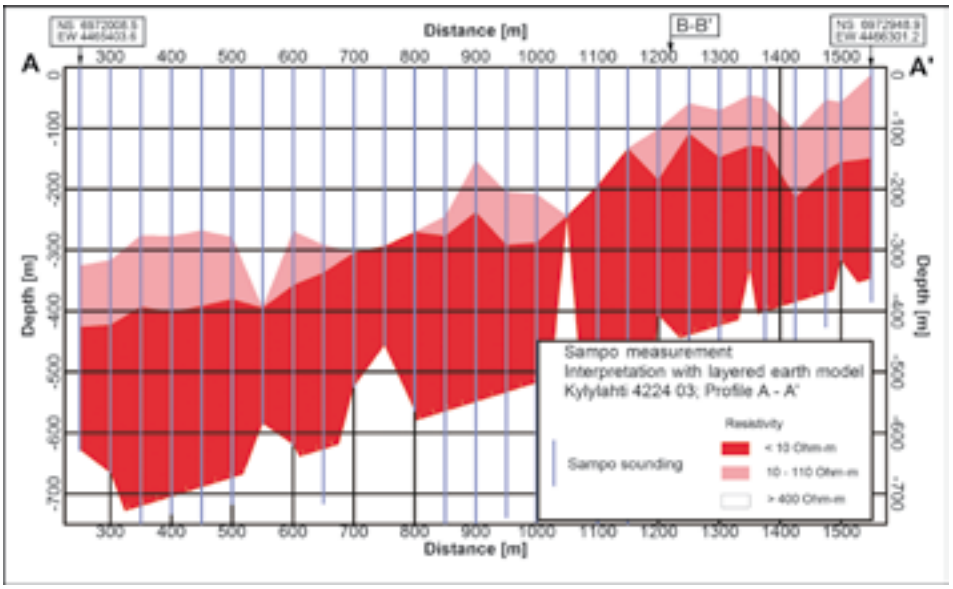

Figure 18. Interpretation of the electromagnetic 'Sampo' measurements along the profile A – A' in Figure 17.

electromagnetic sounding that was carried out with the multifrequency (2 – 20000 Hz) system 'Sampo', described by Soininen et al. (1991). The transmitter used was a horizontal loop with a diameter of 20 – 50 m and the coil separation varying between 300 – 500 metres (in-line configuration). The configurations were both increased to the SW because of known deepening of the conductive anomaly sources. The interpretation of the Sampo profile (A – A' in Figure 17) has been done using the layered earth model (Figure 18). From the figure it can be seen that the conductive horizon (interpreted to be mainly black schists) dips gently (about 20 degrees) towards the SW.

The cross-section geometry of the Kylylahti area profile was further studied using the gravity and magnetic anomaly profiles B – B' in Figure 17, interpreted in Figure 19. Lithological information from the nearest cross section, profile C – C' in Figure 17 was used in the interpretation. The cross-section given in Figure 20 was made by Asko Kontinen in 2004 – 2005. The model parameters adopted from Rekola and Hattula, (1995) are given in Table 5.

The electromagnetic and potential field interpretation given above confirm the basically synformal structure of the Kylylahti area, thus providing a framework for exploration of the ore potential horizons in the zone.

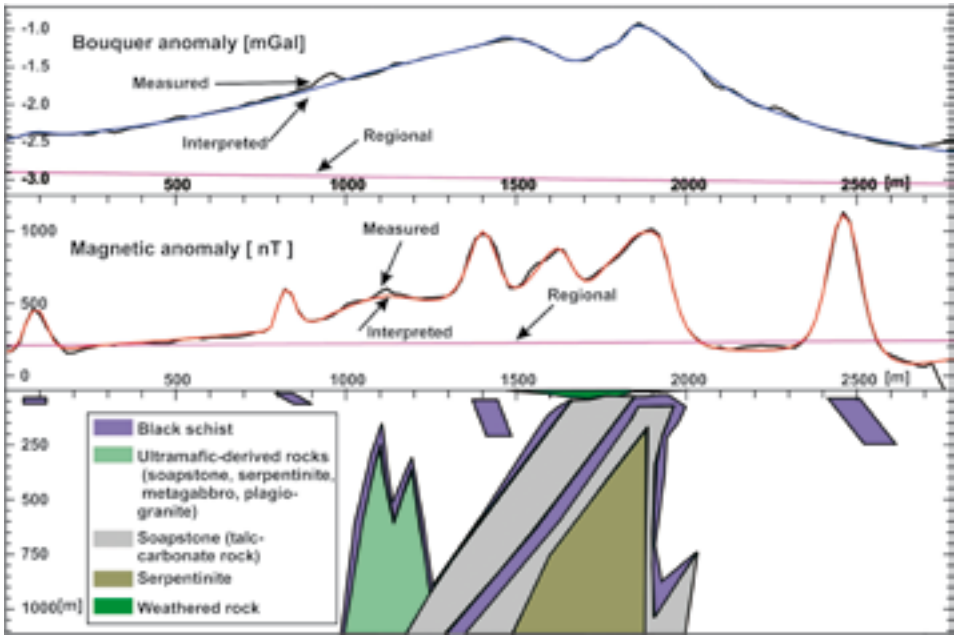

Figure 19. Interpretation of the gravity and magnetic profiles B – B' shown in Figure 17.

Table 5. Rock types and petrophysical parameters used in interpretation (typical values used by Outokumpu Company in parentheses).

Rockname	Density [kg/m^3]	Susceptibility [*10^6 SI]	Remanent magnetization
Mica schist (background)	2750 (2750)	0 (500)	–
Black schist	2930 (2930)	5000 – 30000 (2000 – 60000)	Q = 5 (5–10) D = 70 (70) I = 45 (45)
Soapstone (talc-carbonate rock)	2920 (2920)	17000 – 50000 (3000; 1000 – 500000)	–
Serpentinite (antigorite serpentinite)	2780 (2900)	14000 (20000; 500 – 50000)	–
Soapstone etc (soapstone, serpentinite, metagabbro, plagiogranite)	2900 (2800 – 3000)	25000 (0 – 500000)	–
Tabular bodies (black schists?)	2720 – 2950 **(2600 – 3100)**	5000 – 60000 **(2000 – 60000)**	Q = 0 or 5 (5–10) **D = 70 (70)** I = 45 (45)
Weathered rock	2000	0	–

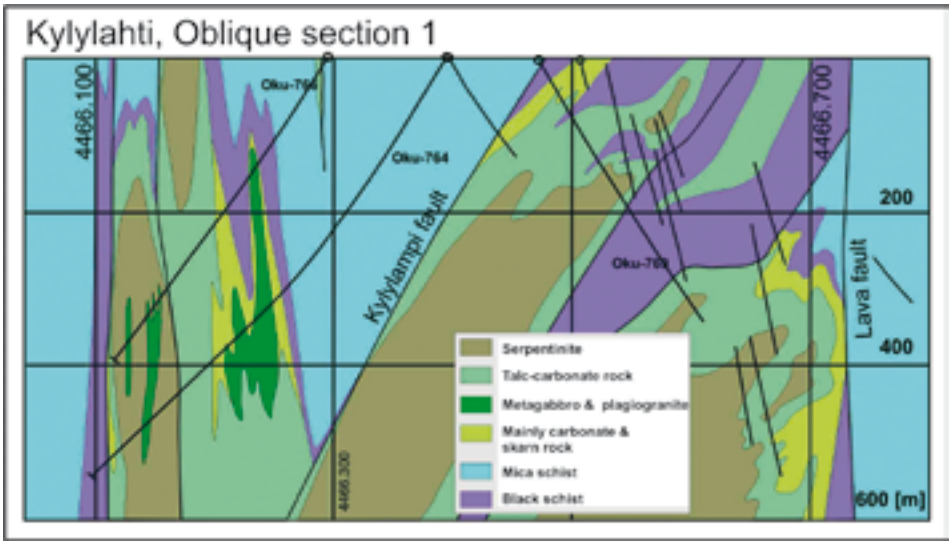

Figure 20. Lithological cross-section along profile C – C' in Figure 17. The dipping black lines show the projected traces of drill holes in the area.

South-west part of the area; Juojärvi anomaly

When interpreting the geometry of the regional structures in the Geomex-area, an important feature is the Juojärvi magnetic anomaly on the SW part of the Outokumpu-Perttilahti (-Kylylahti?) ore potential zone as shown on the magnetic map in Figure 21. In the anomaly zone, a striking feature is its sinuous NW-SE –trend. The geometry of the Juojärvi anomaly zone can be explained by the schematic fold model in Figure 22 where the geometry of the upper edge of the folds emphasized by the blue line, is analogous to that of the Juojärvi magnetic anomaly. The geometry suggests the presence of (at least) two perpenicular regional fold groups in the Juojärvi area, one with a SW-NE trend and another with a SE-NW trending fold axis, as shown in Figure 23. From the geometry of the magnetic anomaly patterns, it can also be concluded that SW-NE folds preceded the SE-NW folds.

The geometry of the main Outokumpu zone is largely defined by the SW-NE trending folds, repre-

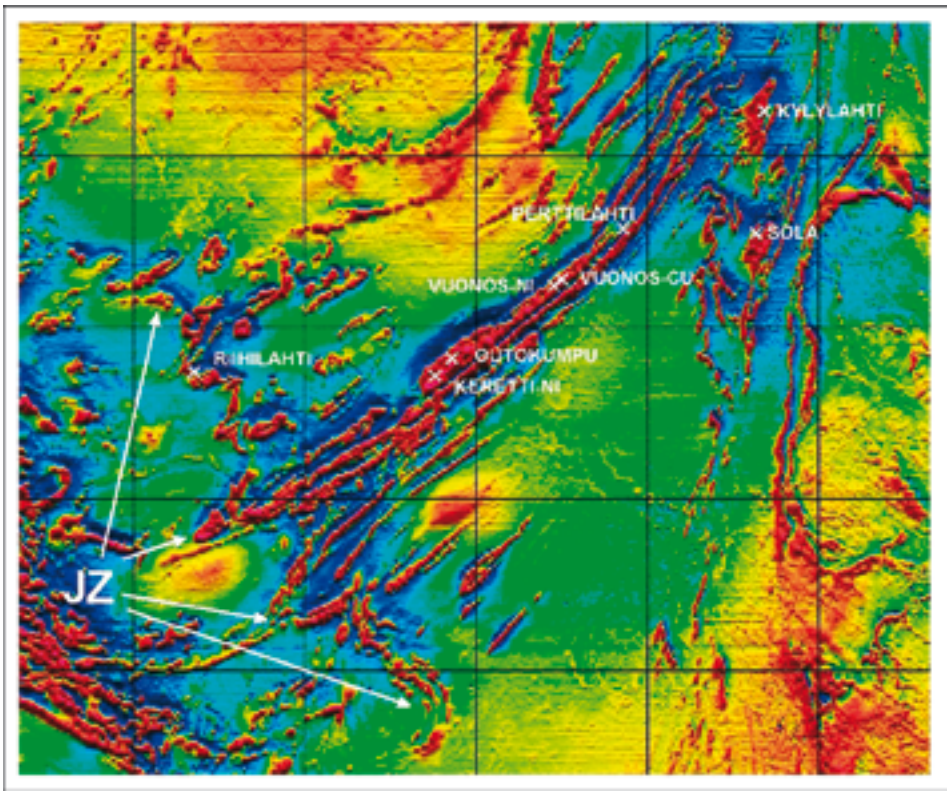

Figure 21.Location of the Juojärvi anomaly zone (JZ) shown on the magnetic low-altitude map.

sented by blue lines for synformal fold axis and red lines for antiforms (Figure 23). The SE-NW folds include the regional synform NE from Juojärvi (SJ) and the more deeply eroded Juojärvi antiform (AJ). The magnetic anomaly zone southwest from antiform AJ in Figure 23. represents the SW limb of the fold, which could therefore potentially contain Outokumpu assemblage rocks. It must also be emphasized that the pattern of the folds in Juojärvi anomaly zone actually reflects the geometry of the vertical cross-section of the SW-NE trending folds, as is evident from the schematic model in Figure 22.

The intersecting SW-NE and SE-NW trending antiforms SW of Juojärvi area can also explain the positions of the Archaean basement windows SW of Juojärvi (see Figure 24). The antiforms interfere at locations emphasized with red circles in Figure 23 and Figure 24 thus generating antiformal domes and exposing the Archaean basement as depicted in Figure 24. In Figure 24c it is evident that the geological dip observations agree with the inferred domal interference patterns.

It must be noted, that Park et al. (1984) have presented an interpretation, where the order of syn- and antiforms is exactly the opposite to that shown in Figure 23. That is to say, they have located the 'domes' in the cores of synforms, and at SJ in Figure 23 in the

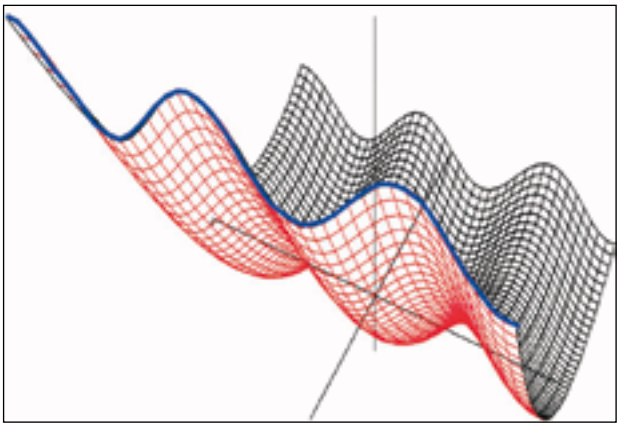

Figure 22. A schematic geometric model to explain the Juojärvi anomaly in Figure 21.

Outokumpu thrust nappe plunges southwest below Juojärvi (AJ), which is not plausible in the light of the geometry of the related anomaly patterns.

In the explanation to the bedrock map of the Heinävesi area Koistinen (1993) concluded that the dome structures are actually thrust slices detached from the basement. However, the interpretation above strongly indicates that interference structures are the main reason for the outcropping 'domes', irrespective

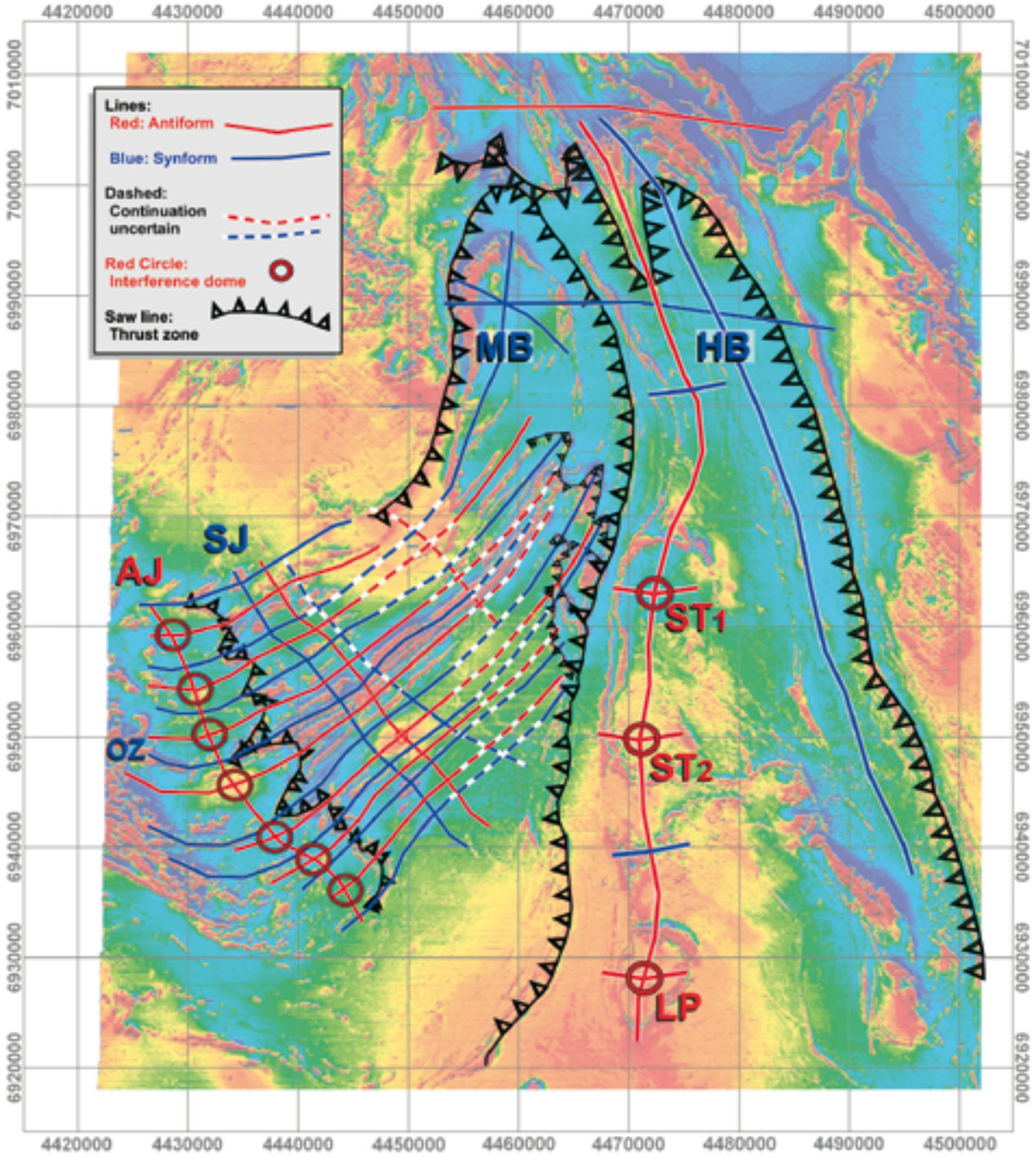

Figure 23. General tectonic features interpreted from geophysical maps of the study area. The base map is the magnetic low-altitude map (see Figure 2 for a more detailed version). OZ = Outokumpu zone regional synform.

of whether they have roots to the basement or not.

The deep seismic reflection profile FIRE-3 (Kukkonen et al., 2006) was measured across the Outokumpu nappe and also trends somewhat obliquely across the SE-part of the Juojärvi anomaly. The segment of the FIRE-3a profile and magnetic map covering the Juojärvi area are shown in Figure 25. From the figure it can be seen that between points B and C, in the middle part of the antiform AJ interpreted above, there are distinct upward convex surfaces. However, at points A and D on the edges of the antiform there are no obvious reflectors, apparently due to the oblique orientation of the seismic profile across the structures. The geometry of the reflection surfaces thus supports the interpretation given in Figure 23; namely the synform-antiform pair SJ – AJ.

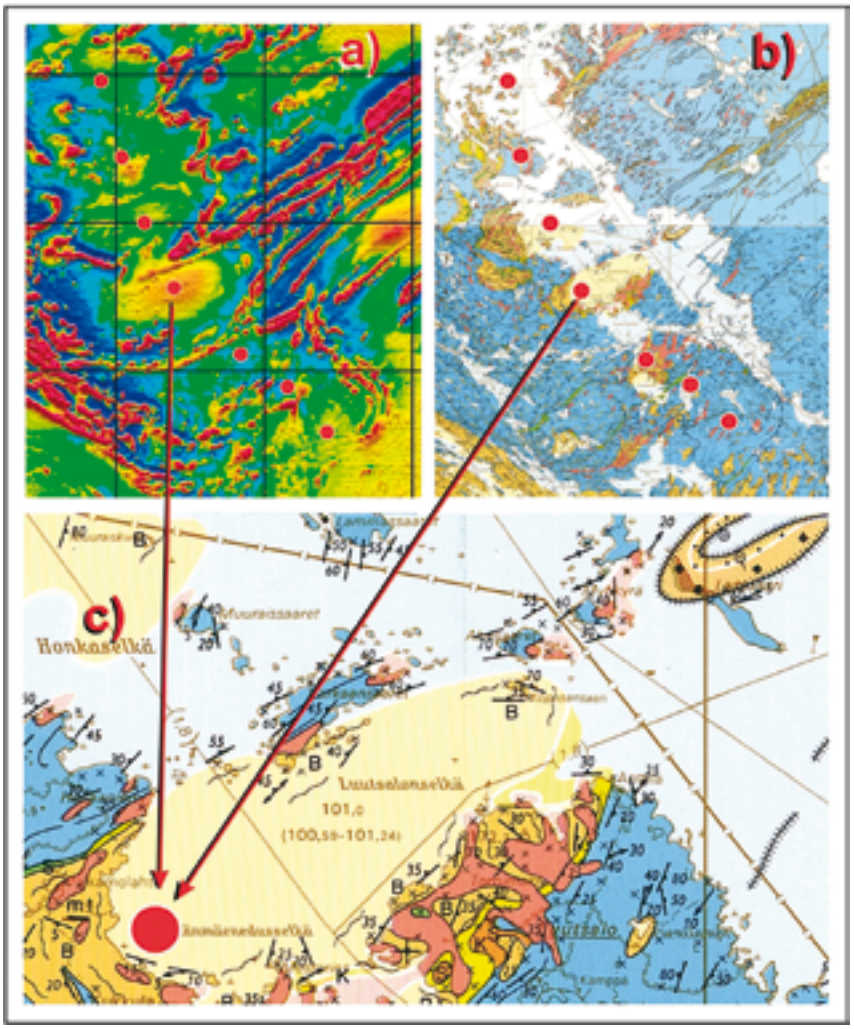

Figure 24. Comparison of the interpreted magnetic interference structures of intersecting antiforms (a) with geology (b and c). The red dots refer to interference points in Figure 23. In (c) an enlarged detail of one of the Archaean basement domes from (b) is shown. The lithological maps in (b) and (c) are from Huhma (1971) and Koistinen (1993).

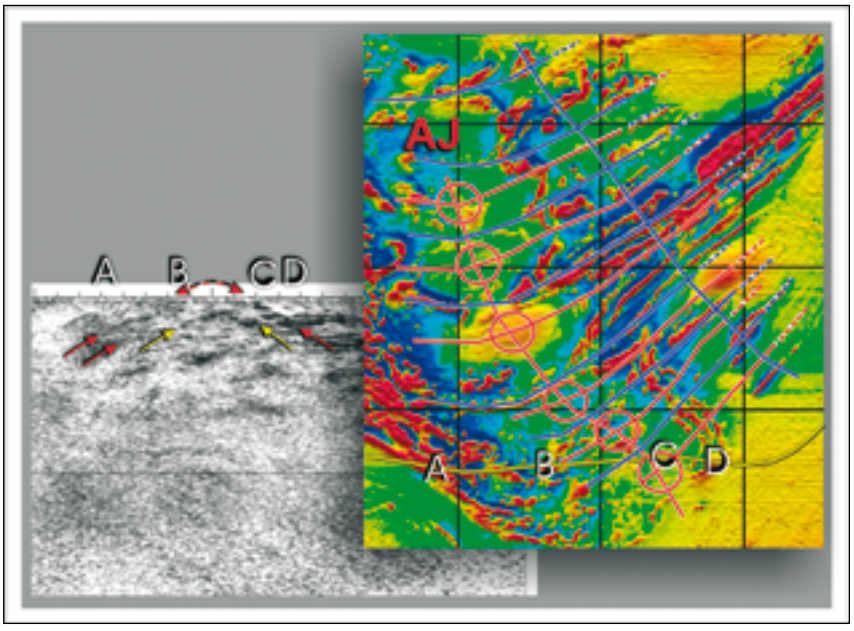

Figure 25. Reflectors in the upper parts of the FIRE-3a deep seismic profile and magnetic low-altitude map of the SW part of the Geomex area. The trend of the FIRE-3a profile is shown by a yellow line on the magnetic map.

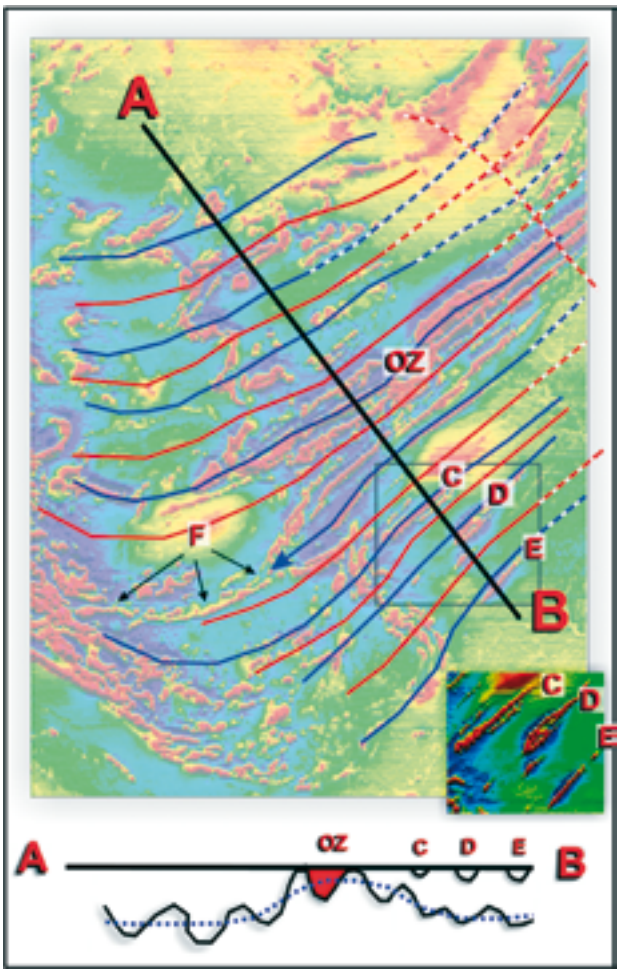

Figure 26. A schematic NW-SE cross-section across the Outokumpu zone area (A – B). Red lines indicate antiforms, blue synforms, OZ = Outokumpu zone. C, D and E = lensoid remnants of higher level layers on upper parts of the deep synforms (shown more clearly on the lower right corner inset). F = continuation of the 'keel' of a synform (blue arrow).

Inspection of the Figure 23 leads to speculation as to why only the main Outokumpu zone synform (OZ in the figure) is outcropping? This is explained in Figure 26, which shows a schematic cross-section of folding across the Outokumpu area, with another longer wavelength component summed with the NE-SW trending folds (blue dotted line in the cross-section). This interpretation is also supported by the deep reflection seismic profile FIRE-3 from Sotkuma dome to Maarianvaara granite considered later.

The lensoid anomalies in Figure 26, e.g. those at points C, D and E represent slices of upper layers remaining on top of the deepest synforms. The minima on their both sides (e.g. on 'D') refer, that they are relatively thin and their disappearance to the NE may relate to shallowing of the basement in that direction. In a similar way at F the 'keel' of the deep synform (marked with blue arrow head in Figure 26) has been preserved in the Juojärvi antiformal ridge (AJ in Figure 23 above).

It must be emphasized that in general, the Outokumpu allochthon consists of discontinuous 'slices' thrusted over each other as described by Park et al. (1983) and Koistinen (1993). Moreover, folding and shear tectonics have been much more complicated than presented here, where only some general regional geometric features are represented. However, as mentioned above, the long, continuous Haaralanniemi anomaly in the electromagnetic in-phase map in Figure 5 demonstrates that despite complicated local scale folding and discontinuous thrusting extensive continuous thrust surfaces are preserved in the lower parts of the Outokumpu allochton (though possibly locally intruded by later plutonites).

Characteristics of anomalies in the central and northern parts of the area

Many of the significant anomalies in the study area can be interpreted using the Juojärvi anomaly described above as a structural analog. For example, the spoon-shaped Miihkali basin in the northern part of the Outokumpu allochthon can also be attributed to interference between two crossing synforms (MB in Figure 23). Furthermore, the Höytiäinen basin (HB) and Outokumpu nappe appear to be separated by a regional antiform structure where the Sotkuma dome (ST1 and ST2) and Liperinsalo dome (LP) are interpreted here as interference structures. Kohonen (1995) who has studied the structure of the Höytiäinen area in detail has inferred a west dipping thrust zone on the eastern side of the Sotkuma dome, cutting the regional Sotkuma-Liperinsalo antiform defined in this paper. This is considered below.

Figure 27 depicts the magnetic anomalies on the eastern flanks of the Höytiäinen basin (HB) and Miihkali basin (MB) and the western flank of the Sotkuma-Liperinsalo antiform (SLA). From the figure it can be seen that at points Gs and Ga there are anomalies visible under the overlying non-magnetic metasedimentary cover (pale green colour) which indicate a gentle westward dip of the linear high anomaly zones on their eastern side. On opposite limbs, such as Gb in Figure 27, no eastward dipping anomaly zones are visible. This lack of symmetry of the anomalies on the flanks of the folds indicates that they are asymmetric, partly overturned to east, which is a further indication of thrusting from the west – south-west.

The geometry of the magnetic interpretation of

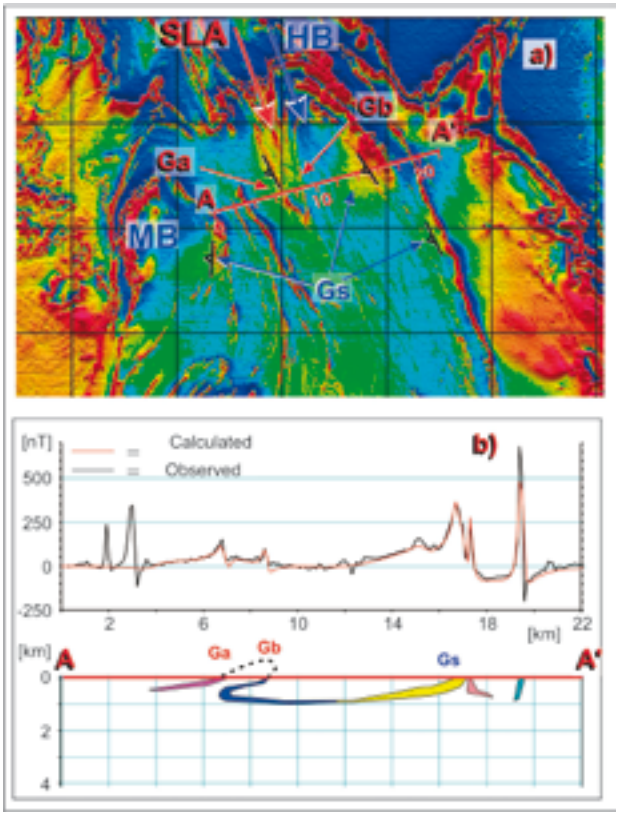

Figure 27. Example of fold dip interpretation for the northern part of the study area. The interpretation of the magnetic profile A – A' is shown in b).

the profile A – A' across the Höytiäinen basin in Figure 27 supports the conclusions above. Variable colours of the model sources refer to slightly different susceptibility values. The interpretation in the figure must be taken as approximate because 2.5 dimensional models have been used, though the geometry is actually three- dimensional. The structures inferred for the Höytiäinen area, between ca. 6–18 km in the profile, are in close agreement with field observations by Kohonen (1995). However, modeling of the Miihkali basin (MB) is more uncertain due to observed strong remanence values in the area (e.g. Rekola and Hattula, 1995).

Regional seismic data

The NE part of the Outokumpu district between Sotkuma dome and Maarianvaara granitoid complex has been surveyed by refraction seismic methods by Outokumpu Oy (Penttilä, 1967). Moreover, the central part of the district has been crossed by the FIRE-3 deep seismic reflection profile (Kukkonen et al., 2006). The profile locations and the reflectors of the refraction profiles are shown in Figure 28.

The seismic refraction profile by Outokumpu Oy in Figure 28 reveals that the base of the Outokumpu nappe is at a depth of ca. 2 kilometers. Moreover, there are dipping reflectors inside the nappe area, probably due to thrust slices reaching the surface. The traces of these surfaces are shown as magnetic highs on the magnetic map in Figure 29.

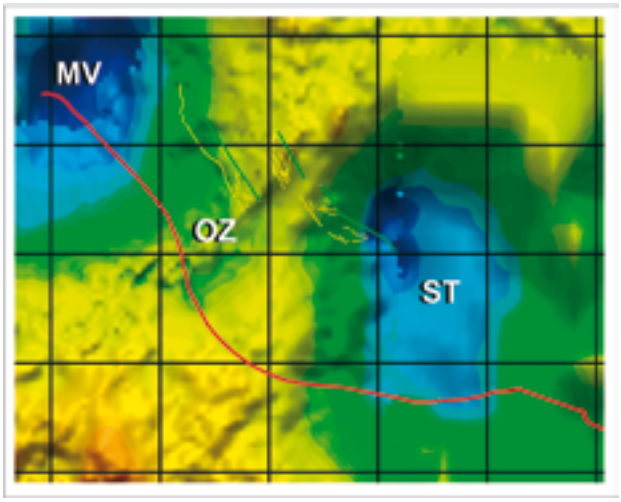

Figure 28. Locations of the NW segment of the FIRE-3 deep seismic reflection profile (red line) and the refraction profiles (green lines). Yellow lines show the main reflectors of the refraction profiles, depths being at map scale. The base map is part of the gravity map shown in Figure 4. MV = Maarianvaara granite minimum, ST = Sotkuma gneiss dome minimum, OZ = Outokumpu zone maximum. The spacing of the coordinate grid lines is 10 x 10 kilometers.

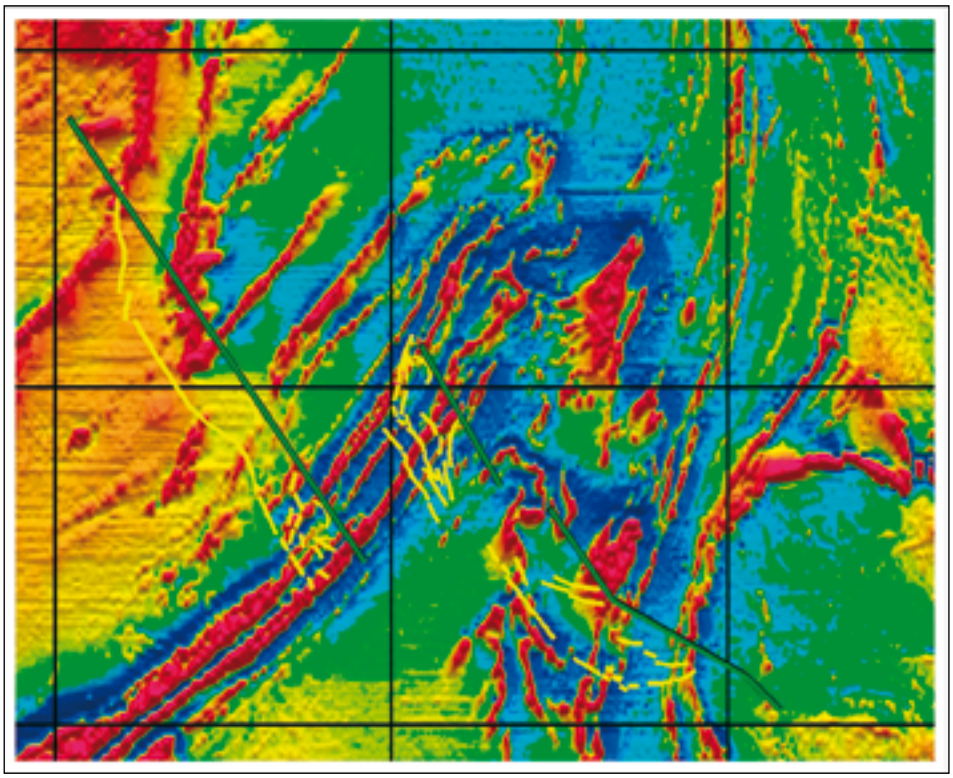

Figure 29. The location and reflectors of the seismic refraction profiles by Outokumpu Oy (Penttilä, 1967). The base map is part of the magnetic map shown in Figure 2.

Regional gravity modelling along the FIRE-3 seismic reflection profile.

In the following we use the geometry of the seismic reflectors for gravity modeling along the FIRE-3 profile shown by the red line in Figure 28. As concluded above, the petrophysical data provided by Outokumpu Mining Oy is not representative of the rock variations of the whole Geomex area, because they have been primarily sampled from drill cores of anomalous ore potential zones. Therefore we use the samples obtained by the Geological Survey of Finland. Sample locations and sub-areas used for density estimation are shown in Figure 13.

The distributions of the densities of samples are shown in Figure 30. Because the density distributions generally have several separate maxima and are biased and thus not normal, the calculated average or mode values of samples are not representative. Therefore, we decided to visually estimate the density values from the modes of the curves.

Maarianvaara granitoid area

The number of samples in the Maarianvaara granitoid area is 46. They are mainly granites and tonalites (33 samples). Some amphibole and mica gneisses (3+3 samples) have also been analyzed. The average and standard deviation of densities of the samples are ca. 2653 kg/m^3 and 127 kg/m^3, correspondingly. The modal density estimated from the main peak in Figure 30 is ca. 2625 kg/m^3.

Outokumpu nappe area

The number of samples from the Outokumpu nappe area is 368. They are mainly mica gneisses (291 samples), although some tonalites, serpentinites, gneisses and granites have also been analyzed (39, 7, 5 and 4 samples respectively). The average and standard deviation of densities of the samples are ca. 2700 kg/m^3 and 51 kg/m^3. The modal density estimated from the main peak in Figure 30. is ca. 2725 kg/m^3.

Sotkuma dome area

The number of samples from the Archaean Sotkuma dome area is 19, mainly gneisses, granodiorites, and granites (9, 5, 2 samples). The average and standard deviation of densities of the samples are ca. 2654

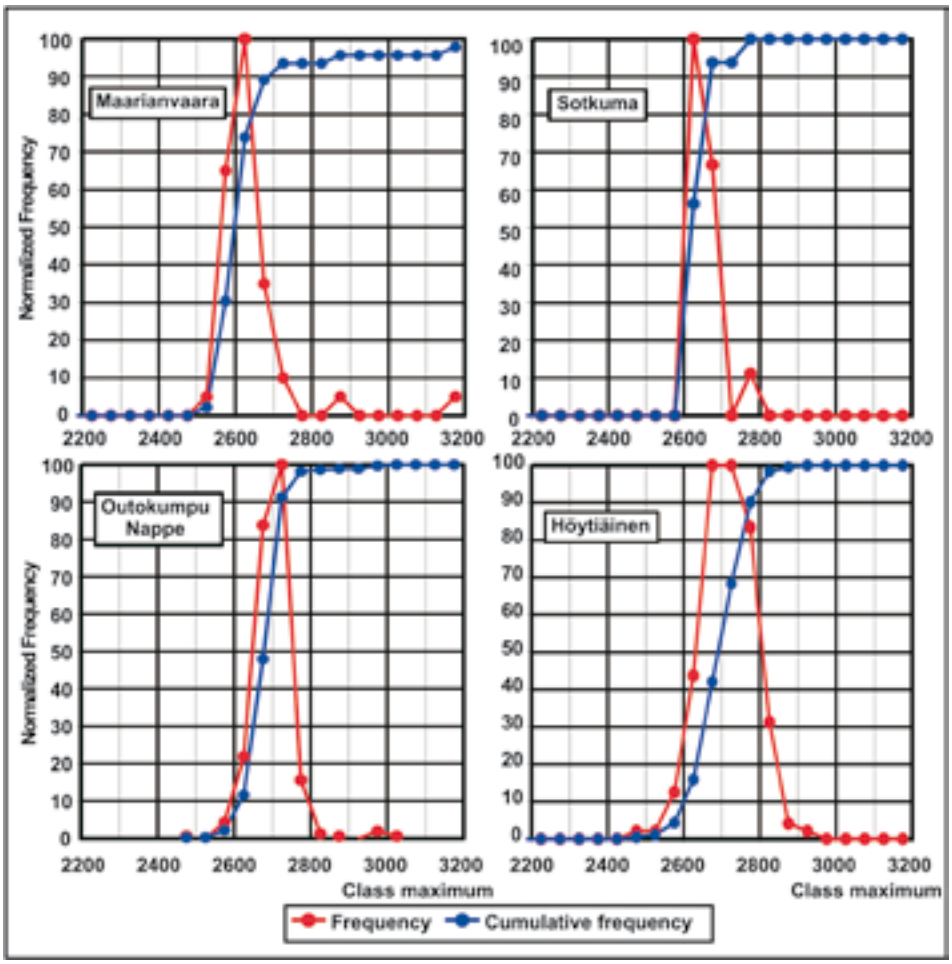

Figure 30. Density distributions of samples of the sub-areas shown in Figure 13.

kg/m^3 and 37 kg/m^3. The modal density estimated from the main peak in Figure 30. is ca. 2630 kg/m^3 (the distribution is biassed towards higher densities compared e.g. to that of Maarianvaara samples).

Höytiäinen area

The number of samples in Höytiäinen area is 183 (symbols overlapping in Figure 13), mainly mica gneisses (169 samples) with some black schists (10 samples). The average and standard deviation of densities of the samples are ca. 2715 kg/m^3 and 70 kg/m^3. The modal density estimated from the relatively broad main peak in Figure 30 is ca. 2700 kg/m^3

The reflectors of the FIRE-3 profile and results of the gravity interpretation along the profile are shown in Figure 31. The gravity anomaly profile has been combined from the regional and local scale grids used for compiling the gravity map in Figure 4. Therefore, there are discontinuities at both ends of the profile (indicated by question marks). The coloured horizontal arrows show the boundaries of the blocks defined from the geological maps of the area. The surfaces used for modelling the geometry of the anomaly sources were selected from the FIRE-3 profile using reflectors outcropping at the geological contacts.

The gravity modelling has been made using 2.5 dimensional sources assuming the profile as a straight line. The interpreted model sources and their densities are given in Figure 31a; the half widths of the sources are given in parentheses. It must be emphasized that at both ends at Maarianvaara and Sotkuma the models are most uncertain due to low quality of the data.

The gravity models based on the geometry of the seismic reflectors in Figure 31 suggest that the base of the Outokumpu nappe (mainly mica schists, blue in the figure) varies between depths of ca. 2–6 kilometers. The contact area between Outokumpu nappe and Sotkuma dome is more uncertain due to the poor quality of the data. Moreover, it appears, that Maarianvaara granitoid underlies the western part of the Outokumpu nappe. The Outokumpu Deep Drilling

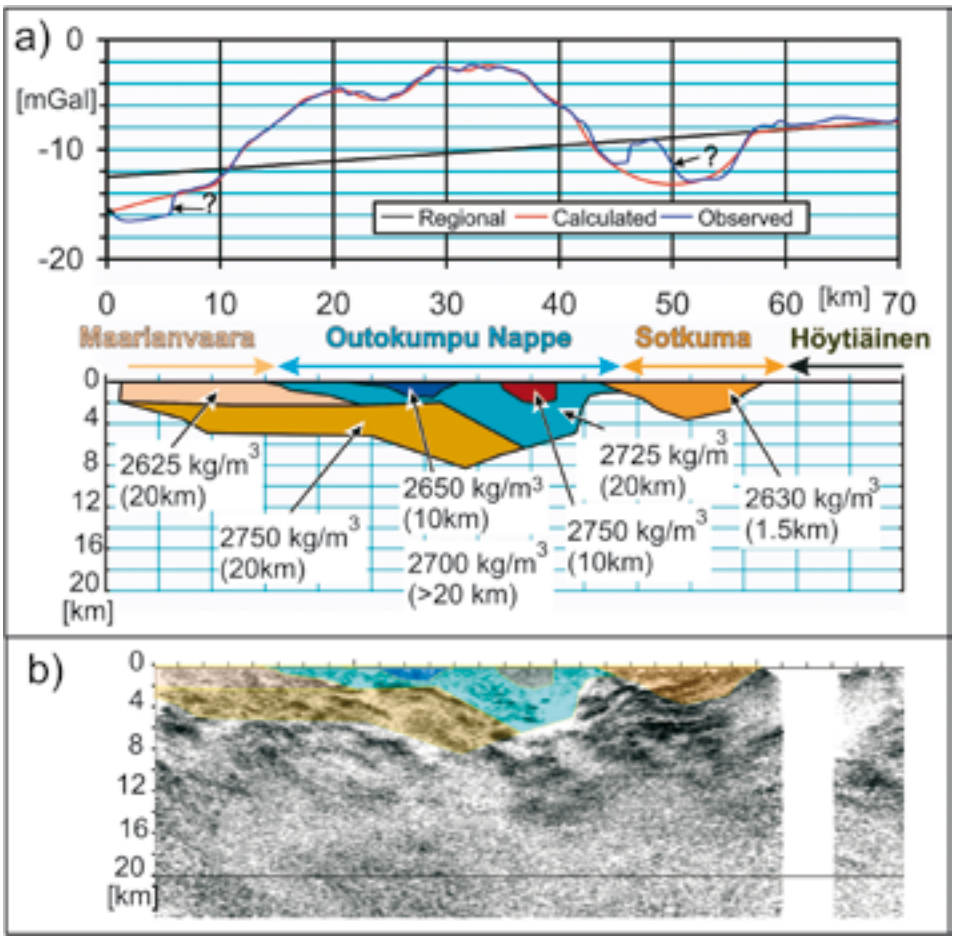

Figure 31. Comparison of the 2.5D gravity interpretation (a) with seismic FIRE-3 reflection profile (b). For each model block is given the density and half widths. The gravity 'anomalies' between ca. 0 – 7 km and 45–53 km are probably due to errors in levelling between regional and local scale gravity data.

Project carried out by GTK (Kukkonen, 2006) has drilled a ca. 2 km deep hole on the SE side of the main Outokumpu zone ('X' in Figure 13). The lowest parts of the drilling penetrated pegmatitic granite at depths below ca. 2.0 km, which are possibly correlative with the Maarianvaara granites.

The geometry of the Sotkuma dome remains uncertain, though the calculated anomaly appears quite realistic. The reflectors inside the dome could be explained by higher density layers (ca 2780 kg/m^3) or fractures due to thrusting from the W-SW, as suggested above.

The high density (2750 kg/m^3) source rocks within and below the Outokumpu nappe were evaluated by considering 2745 – 2754 kg/m^3 density range rocks in the GTK petrophysical database. The majority of samples (49 samples of 67 = ca. 73%) in this range are various types of mica gneisses, the remainder being mainly tonalites. In the Outokumpu drill hole data base there are 392 samples in the 2750 kg/m^3 class (± 5 kg/m^3) of which 237 samples (ca 60%) are mica schists or mica gneisses. The other samples were mainly various types of black schists (11%), quartzites (ca. 9%) and serpentinites (ca. 7%). It must be emphasized that the higher density zone below the Outokumpu block could possibly be substituted also by multiple thin layers of higher density rocks of the Outokumpu association. This possibility was demostrated by the Outokumpu Deep Drilling Project which penetrated Outokumpu association rocks having bulk density of ca. 2760 kg/m^3 between depths of ca. 1300 – 1500 m in the area. The low density zone with density 2650 kg/m^3 close to the major Outokumpu anomaly zone might be due to thicker soil cover in the area (not verified in this project).

Comparison of gravity interpretation with the seismic reflection in Figure 31 demonstrates that using the modal densities of the sub-areas, the geometry of seismic profile reflectors can satisfactorily explain the main gravity variations.

Where are the ore bodies?

For almost a century the Outokumpu area has been very intensively drilled, sampled and studied by numerous geological, geophysical and geochemical methods, thus making it unlikely, or at least difficult to find any new economic occurences in the area. However, we consider the following points relevant with respect to future exploration work:

- The long wavelength magnetic map in Figure 3 effectively discriminants areas where orebodies and mineralizations are concentrated (and where conversely, they are not concentrated).
- The uranium – thorium -ratio shows an increase in ore potential areas, as in Figure 9.
- By combining long wavelength magnetic anomalies with high U/Th anomalies it is possible to define potential exploration targets with greater accuracy, as is demonstrated in Figures 10 and 11.
- The petrophysical database for the Outokumpu Mining Oy samples can be used to define the susceptibility – density combinations of the most enriched samples, as is demonstrated in Figures 15.
- At regional scale, the general geometry of the Outokumpu nappe forms a large basin within which the prospective Outokumpu assemblage outcrops in association with thrusts. This basin structure and its margins are obviously most interesting, while additional prospective areas may still be present in Outokumpu assemblage occurrences, such as at Kylylahti and Sola (in Figure 21). Moreover, the Juojärvi anomaly shown in Figure 21 is also of interest, in that the base of the main Outokumpu zone evidently outcrops there, too. Finally, the long Haaralanniemi anomaly shown in Figure 5 is worth closer investigation.

Figure 32 shows two possible targets for future prospecting. Both of them are associated with outcropping margins of the Outokumpu nappe system and high gravity anomalies. The Juojärvi anomaly (JJ) is partly beneath the lake, but partly on dry land. The Leppälahti anomaly has been drilled, but missing the gravity high locating NW from the drill holes.

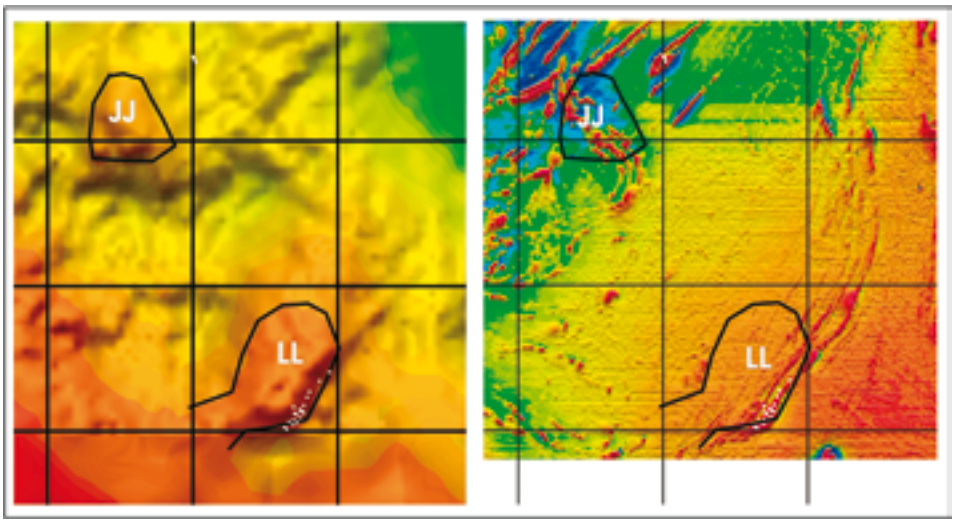

Figure 32. Possible targets for future prospecting, namely the gravity and magnetic anomalies of JJ (Juojärvi) and LL (Leppälahti) areas. Respective locations are shown in the magnetic map in Figure 2. The white dots show locations of drillholes.

Conclusions

The detailed analysis of geophysical and petrophysical data from the Outokumpu area carried out during the Geomex project reveals many lithological, tectonic, and petrophysical characteristics, which are useful for future exploration in the area. The long-wavelength magnetic maps as such effectively delineate rock horizons that are already known to have potential for Outokumpu type mineralizations. Combined with radiometric U/Th data the magnetic maps can be used for defining the future target areas in more detail. Moreover, electromagnetic maps are useful in outlining the major structures in the study area. Combined with the magnetic data, the electromagnetic in-phase data can be used for defining areas dominated by conductive pyrrhotite bearing black schists and non-conductive rocks containing magnetite.

The petrophysical data obtained by GTK and Outo-

kumpu Mining Oy have been classified according to their susceptibility and density values. This analysis showed that even in a single rock type there may be several characteristic susceptibility-density -associations reflecting significant variations in accessory minerals (including ore minerals).

The qualitative and quantative analysis of geophysical maps and data show that large scale fold interference patterns are present which, in connection with the thrust structures, reflect the regional geometry of the structures of the Outokumpu nappe area.

In summary, we conclude that the detailed geophysical studies in the Geomex project offer several geophysical and petrophysical indicators that can be utilized in future detailed ore prospecting studies in the area.

REFERENCES

Airo, M-L. and Loukola-Ruskeeniemi, K., 2004. Characterization of sulfide deposits by airborne magnetic and gamma-ray responses in eastern Finland. Ore Geology Reviews 24 (2004) 67–84.

Claesson, S., Huhma, H., Kinny, P.D., and Williams, I.S., 1993. Svecofennian detrital zircon ages – implications for the Precambrian evolution of the Baltic Shield. Precambrian Res. 64, 109–130.

Elo, S. 1997. Interpretations of the Gravity Anomaly Map of Finland. Geophysica, 33–19, 51–80.

Gaál, G., Koistinen, T., Mattila, E. 1975. Tectonics and stratigraphy of the vicinity of Outokumpu, North Karelia, Finland : including a structural analysis of the Outokumpu ore deposit. Geological Survey of Finland. Bulletin 271. 67 p. + 6 app. maps.

Hautaniemi, H.; Kurimo, M.; Multala, J.; Leväniemi, H.; Vironmäki, J. 2005. The „Three In One" aerogeophysical concept of GTK in 2004. In: Airo, M.-L. (ed.) Aerogeophysics in Finland 1972–2004 : methods, system characteristics and applications. Geological Survey of Finland. Special Paper 39, 21–74.

Huhma, A. 1971. Kallioperäkartta – Pre-Quaternary rocks. Lehti – Sheet 4222, Outokumpu. Suomen geologinen kartta – Geological map of Finland 1 : 100 000.

Kääriäinen, J. and Mäkinen, J., 1997. The 1979–1996 gravity survey and results of the gravity survey of Finland 1945–1996. Publications of the Finnish Geodetic Institute, N:o 125, 24 pages.

Kivekäs, L. 1974. Maankuoren radioaktiivisuudesta ja gammasäteilyn laboratoriomittauksista. In: Petrofysiikka S-3. Helsinki University of Technology, Department of Mining and Metallurgy, Otaniemi, Finland. Unpublished report (in Finnish)

Kohonen, J. 1995. From continental rifting to collisional crustal shortening – Paleoproterozoic Kaleva metasediments of the Höytiäinen area in North Karelia, Finland. Geological Survey of Finland. Bulletin 380. 79 p. + 1 app.

Koistinen, T. J. 1981. Structural evolution of an early Proterozoic stratabound Cu-Co-Zn deposit, Outokumpu, Finland. Transactions of the Royal Society of Edinburgh: Earth Sciences 72 (2), 115–158.

Koistinen, T. 1993. Heinäveden kartta-alueen kallioperä. Summary: Pre-Quaternary rocks of the Heinävesi map-sheet area. Suomen geologinen kartta 1 : 100 000 : kallioperäkarttojen selitykset lehti 4221. 64 p.

Kontinen, A., Peltonen, P. 2002. Geomex; Modelling of the Outokumpu type semimassive sulphide deposits. A summary of the results and conclusions of the modelling subproject. Unpublished report. Geological Survey of Finland.

Kontinen, A., Peltonen, P. 2003. Description and genetic modelling of the Outokumpu type rock assemblage and sulphide ores – a GEOMEX subproject. GEOMEX / Preliminary Technical Report. Geological Survey of Finland.

Korhonen, J. 1980. The aeromagnetic map of Finland 1:2 000000. Geological Survey of Finland.

Korsman, K.; Koistinen, T.; Kohonen, J.; Wennerström, M.; Ekdahl, E.; Honkamo, M.; Idman, H.; Pekkala, Y. 1997 (editors). Suomen kallioperäkartta = Berggrundskarta över Finland = Bedrock map of Finland 1 : 1 000 000. Geologian tutkimuskeskus. Erikoiskartat, Special maps 37 ISBN 951-690-691-5

Kukkonen, I.T. 2006. Outokumpu Deep Drilling Project: First results and status of research. Abstract in: 27th Nordic Geological Winter Meeting, Oulu, 9.–12.01.2006. Bulletin of the Geological Society of Finland, Special Issue 1, 2006.

Kukkonen, I.T.; Heikkinen, P.; Ekdahl, E.; Hjelt, S.-E.; Korja, A.; Lahtinen, R.; Yliniemi, J. and FIRE Working Group. 2006. FIRE reflection seismic transects: New images of the crust in the Fennoscandian Shield. Abstract in: 27th Nordic Geological Winter Meeting, Oulu, 9.–12.01.2006. Bulletin of the Geological Society of Finland, Special Issue 1, 2006.

Lehtonen, T. 1981. Outokummun alueen kivilajien petrofysikaalisista ominaisuuksista. On petrophysical properties of rocks in Outokump area (In Finnish). Unpubl. thesis, University of Technology, Helsinki, Finland. 77 p.

Mäkelä, Markku 1974. A study of sulfur isotopes in Outokumpu ore deposit, Finland. Geological Survey of Finland. Bulletin 267. 45 p.

Park, A. F., Bowes, D. R., Halden , N. M. and Koistinen, T. J. 1984. Tectonic evolution at an early Proterozoic continental margin: the Svecokarelides of eastern Finland. Journal of Geodynamics. 1, 359–386.

Peltoniemi, M. 1982. Characteristics and results of an airborne electromagnetic method of geophysical surveying. Geological Survey of Finland. Bulletin 321. 229 p.

Peltoniemi, Markku 2005. Airborne geophysics in Finland in perspective. In: Airo, M.-L. (ed.) Aerogeophysics in Finland 1972–2004 : methods, system characteristics and applications. Geological Survey of Finland. Special Paper 39 , 7–20.

Penttilä, E. 1967. Outokumpujakson räjäytysseismologisesta tutkimustyöstä. On the seismological study of the Outokumpu zone. Report by Outokumpu Oy (in Finnish).

Rekola, T., Hattula, A. 1995. Geophysical surveys for strata-bound Outokumpu-type Cu-Co-Zn deposits at Kylylahti, eastern Finland. In: Conference papers from the ASEG 11th Geophysical Conference and Exhibition, Adelaide, 3–6 September 1995. Exploration Geophysics 26 (2–3), 60–65.

Ruotoistenmäki, T., Tervo, T. 2004. Geomex-Geophysics: Final report: Geophysical regional and local scale data, maps and interpretation. Petrophysical summary and data. Unpublished project report. Geological Survey of Finland.

Soininen, H. and Jokinen, T. 1991. Sampo, a new wide-band electromagnetic system. European Association of Exploration Geophysics 53rd meeting and Technical Exhibition, Florence,

Italy. Technical programme and Abstracts of papers, 366 – 367.

Sorjonen-Ward, Peter 1997. An overview of the geological and tectonic evolution of eastern Finland. In: Loukola-Ruskeeniemi, K. & Sorjonen-Ward, P. (eds.) Research and exploration – where do they meet? 4th Biennial SGA Meeting, August 11–13, 1997, Turku, Finland. Excursion guidebook A4: ore deposits in eastern Finland. Geologian tutkimuskeskus. Opas 42, 11–22.

Sorjonen-Ward, P., Luukkonen E. J., 2005. Archean rocks. In: Lehtinen, M., Nurmi, P. A., Rämö, O. T. (Eds.), 2005. Precambrian Geology of Finland – Key to the Evolution of the Fennoscandian Shield. Developments in Precambrian Geology ; 14: , xiv, 736 s. Elsevier B.V., Amsterdam, pp 19–99. ISBN 0-444-51421-X

Trüstedt, O. 1921. Över geologin inom Outokumpu området, discussion. (In Swedish): Meddelande från Geologiska Föreningen i Helsingfors år 1919–1920, 16.

Tyni, M., Parkkinen, J., Mäkelä, M., Pekkarinen, L., Loukola-Ruskeeniemi, K., Kuronen, E,. Tuokko, I., 1997. Outokumpu district. In: Loukola-Ruskeeniemi, K. & Sorjonen-Ward, P. (eds.) Research and exploration – where do they meet? 4th Biennial SGA Meeting, August 11–13, 1997, Turku, Finland. Excursion guidebook A4 : ore deposits in eastern Finland. Geologian tutkimuskeskus. Opas 42, 23–41.

Tätä julkaisua myy

GEOLOGIAN TUTKIMUSKESKUS (GTK)
Julkaisumyynti
PL 96
02151 Espoo
☎ 020 550 11
Telekopio: 020 550 12

GTK, Itä-Suomen yksikkö
Kirjasto
PL 1237
70211 Kuopio
☎ 020 550 11
Telekopio: 020 550 13

GTK, Pohjois-Suomen yksikkö
Kirjasto
PL 77
96101 Rovaniemi
☎ 020 550 11
Telekopio: 020 550 14

Sähköposti: julkaisumyynti@gtk.fi
www.gsf.fi

Denna publikation säljes av

GEOLOGISKA FORSKNINGSCENTRALEN (GTK)
Publikationsförsäljning
PB 96
02151 Esbo
☎ 020 550 11
Telefax: 020 550 12

GTK, Östra Finlands enhet
Biblioteket
PB 1237
70211 Kuopio
☎ 020 550 11
Telefax: 020 550 13

GTK, Norra Finlands enhet
Biblioteket
PB 77
96101 Rovaniemi
☎ 020 550 11
Telefax: 020 550 14

ISBN 951-690-959-0
ISSN 0781-4240

This publication can be obtained from

GEOLOGICAL SURVEY OF FINLAND (GTK)
Publication sales
P.O. Box 96
FI-02151 Espoo, Finland
☎ +358 20 550 11
Telefax: +358 20 550 12

GTK, Eastern Finland Office
Library
P.O. Box 1237
FI-70211 Kuopio, Finland
☎ +358 20 550 11
Telefax: +358 20 550 13

GTK, Northern Finland Office
Library
P.O. Box 77
FI-96101 Rovaniemi, Finland
☎ +358 20 550 11
Telefax: +358 20 550 14

9 789516 909595